NASA

National Aeronautics and
Space Administration

CONCEPTUAL DESIGN, EVALUATION AND RESEARCH IDENTIFICATION FOR REMOTE AUGMENTED PROPULSIVE LIFT SYSTEMS (RALS) WITH EJECTORS FOR VTOL AIRCRAFT

Final Report

By

W.S. Willis
M. Konarski
W.V. Sutherland

GENERAL ELECTRIC COMPANY

May 1982

Prepared for

National Aeronautics and Space Administration
LEWIS RESEARCH CENTER
21000 BROOKPARK ROAD
CLEVELAND, OHIO 44135

Contract NAS3-22042

ERRATA

NASA Contractor Report 165906
General Electric Company Report R82AEB315

CONCEPTUAL DESIGN, EVALUATION AND RESEARCH IDENTIFICATION FOR REMOTE AUGMENTED PROPULSIVE LIFT SYSTEMS (RAPLS) WITH EJECTORS FOR VTOL AIRCRAFT

W. S. Willis, M. Konarski, and W. V. Sutherland
May 1982

Cover and report documentation page: The NASA report number should be CR-167906.

1 Report No [redacted] CR-167906	2. Government Accession No.	3. Recipient's Catalog No.
4 Title and Subtitle CONCEPTUAL DESIGN, EVALUATION AND RESEARCH IDENTIFICATION FOR REMOTE AUGMENTED PROPULSIVE LIFT SYSTEMS (RALS) WITH EJECTORS FOR VTOL AIRCRAFT - FINAL REPORT		5. Report Date May 1982 6. Performing Organization Code
7 Author(s) W.S. Willis, M. Konarski, and M.V. Sutherland		8. Performing Organization Report No R82AEB315 10. Work Unit No.
9. Performing Organization Name and Address General Electric Company Aircraft Engine Business Group Cincinnati, OH 45215		11. Contract or Grant No. NAS3-22042 13. Type of Report and Period Covered Contract Final Report
12. Sponsoring Agency Name and Address National Aeronautics and Space Administration Washington, D.C. 20546		14. Sponsoring Agency Code

15. Supplementary Notes

Project Manager, R. Woolett, NASA-Lewis Research Center, 21000 Brookpark Road, Cleveland, OH 44135

16. Abstract

This report covers a study of ejector concepts for use with a Remote Augmented Lift System (RALS) exhaust nozzle. A number of concepts were considered and three were selected as having the greatest promise of providing the desired aircraft and exhaust gas cooling and lift enhancement. A scale model test program is recommended to explore the effects of the more important parameters on ejector performance.

17 Key Words (Suggested by Author(s))	18. Distribution Statement
Remote Exhaust Nozzle Remote Augmented Lift Systems (RALS) Ejector Vertical Takeoff (VTO) Aircraft	

19 Security Classif (of this report)	20. Security Classif (of this page)	21. No. of Pages	22 Price*
Unclassified	Unclassified		

* For sale by the National Technical Information Service, Springfield, Virginia 22161

TABLE OF CONTENTS

LIST OF ILLUSTRATIONS

LIST OF ILLUSTRATIONS (Concluded)

LIST OF TABLES

1.0 SUMMARY

This report covers a study conducted by the General Electric Company to evaluate new concepts in Remote Augmented Lift Systems (RALS) to improve their installation characteristics. The RALS propulsive lift system operates by extracting most of the bypass airflow from a turbofan engine and ducting it forward in the aircraft, through a remote augmentor and vectored exhaust nozzle. This system provides a lift vector forward of the aircraft center of gravity to facilitate control and balance of the aircraft in the vertical (VTO) mode of operation.

This study explored a variety of concepts adding ejectors to the remote exhaust nozzle to cool the aircraft compartment, mix and cool the exhaust footprint, and to achieve some thrust (lift) enhancement within practical geometric limitations. A number of ejector concepts were evaluated and three were selected for detailed study.

Due to the lack of applicable test data, exact performance predictions for the selected concepts were not possible. Using analytical methods developed for other ejectors, the critical performance parameters were identified; and a scale model test program was recommended to explore the effects of the more important parameters on performance of the selected ejector concepts.

2.0 INTRODUCTION

The RALS concept has been proposed by General Electric as a means to supply a controllable forward lift vector in a V/STOL aircraft. The concept has been evaluated under contracts from the Naval Air Propulsion Center (References 1, 2, 3, and 4). These studies showed that, compared to propulsion systems using dedicated lift engines, the RALS system can provide about the same size (TOGW) supersonic fighter aircraft to complete the specified deck-launched intercept mission. However, since all of the installed turbomachinery is available to provide forward thrust, the RALS-powered aircraft far exceeds other concepts in terms of supersonic acceleration and combat specific energy, P_s. It also results in a much lower life cycle cost because only one type of engine must be developed, procured, and maintained.

While these are important advantages, the RALS system does have disadvantages in that the remote augmentor is located near the pilot's compartment and electronics bay, requiring a means of local cooling, and it results in a relatively high exhaust gas temperature with potential deck heating problems.

In theory, the use of an ejector nozzle in the remote system could pump sufficient ambient air to cool the surrounding aircraft bay and to mix the exhaust stream to a lower average footprint temperature. In addition, some degree of lift enhancement might be possible. In practice, the geometric constraint placed on the ejector for stowage and for low drag in the supersonic flight mode would make the use of a highly complex and highly efficient ejector quite difficult. However, if sufficient ejector action could be provided to increase the lift vector enough to offset the weight increase, the cooling advantages could still make the concept worthwhile.

Since the geometric constraints of the installation were found to be a strong driver in the selection of desirable concepts, special attention was paid to establishing representative design requirements. A number of aircraft companies that had studied RALS-powered aircraft designs provided inputs as to thrust split, vectoring and modulation needs, space availability, and installation constraints. Because of differences in the aircraft designs, a rather wide range of installation requirements resulted.

Concurrent with this study, General Electric was performing contract NAS2-10556 from NASA-Ames to redesign their large scale VEO fighter model (Figure 1) to simulate a RALS propulsion system. This redesign consisted of adding a third J97 engine mounted in the fuselage with its exhaust supplying a remote exhaust nozzle near the nose of the model. In consideration of the difficulty encountered in developing other ejectors, particularly with respect to scaling, it was felt to be highly desirable that the option remain open to test any attractive concept in a larger size. The decision was therefore made to configure the selected ejectors to meet the geometric constraints of the VEO model. Thus, if the results of a small-scale model tested with a facility air supply prove to be sufficiently attractive, a larger scale model could

Figure 1. NASA-Ames Large-Scale VEO Fighter Model.

subsequently be tested in the VEO model at Ames. This decision narrowed the range of installation requirements to those of a single aircraft concept; and although the results of ejector development would be less generic in nature, the potential of large scale tesing was felt to outweigh this disadvantage.

3.0 DESIGN STUDY

The initial task of the study consisted of establishing design requirements. This was followed by a review of analytical methods, the identification of a number of design concepts, and the selection of three specific concepts worthy of further detailed study. Layouts were prepared of the selected concepts and model requirements were determined as needed to investigate the effect of key design parameters on performance of the selected concepts.

3.1 REQUIREMENTS AND GOALS

To establish meaningful design requirements for the study, the following aircraft companies were contacted:

- General Dynamics, Fort Worth Division
- Grumman Aerospace Company
- McDonnell Douglas Aircraft Company
- Northrop Corporation
- Vought Corporation

Each of the companies had previously worked with supersonic fighter aircraft designs using RALS propulsion systems. In addition, Mr. T. Miller of the Naval Air Development Center provided information from his in-house studies. The inputs received from these sources did not provide a consensus of requirements, but did provide a range from which design goals could be established. Table I shows the principal parameters affecting the design of ejectors as received from these sources.

One of the aircraft designs was a single-engine configuration; others used two engines. One design used two engines supplying a single remote burner and nozzle. In general, the designs having the remote nozzle located just behind the pilot required a 45/55 thrust split (remote main nozzle) and those having the nozzle ahead of the pilot required about 35/65 thrust split.

In terms of the fuselage space available for the remote burner and nozzle, Figure 2 summarizes the geometric requirements.

Because of the diversity in requirements among the different aircraft designs, a single design goal could not be set for all ejectors. Instead, several categories were established to cover the range of possible designs. Figure 3 illustrates the usual method of presentation of ejector performance.

Table I. Results of Industry Survey.

Aircraft Company	Vector Angle (X-Y) Degree Fwd/Aft	Vector Angle (Side) degree	Bay Temp., degree	Thrust Mod., %	Thrust Ratio Front-Rear
A	15 30	± 15	420	Not Specified	35/65
B	20 45	± 15 to 35	Cooling Air Required	± 7 pitch	35/65
C	15 60	± 10	?	± 25 landing ± 20 T.O.	39 - 61 41 - 59
D	15 35	± 6	800 for Ti 550 for Composites	± 10	45 - 55 55 - 45
E	20 30	± 15	T_{Bay} Low Enough for Insulated Composites	± 9.2	40/60
NADC	0 90	± 10	Not Specified	± 10	32/68

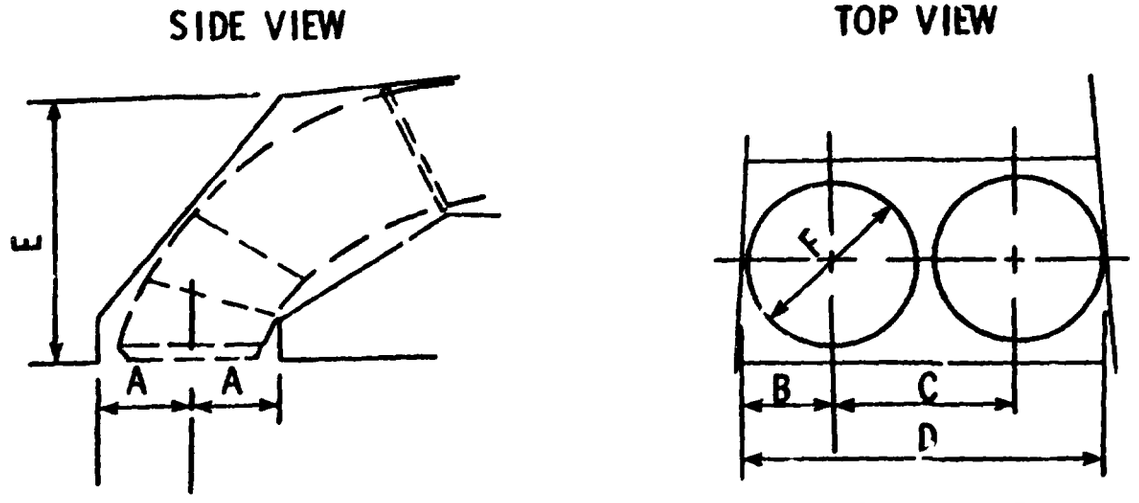

AIRFRAMER	NO. OF ENGINES	A IN.	B IN.	C IN.	D IN.	E IN.	F IN.	BASE AREA FT^2
A	2	20	14	27	55	40	24	15.3
B	1	15.6	19.2	-	38.4	40	24	8.32
C	2	20	14	30	58	60	24	16.1
D	2	15	15.6	27.2	58.4	48	23	12.2
AVG. INST.	2	20	14-15	27	58	40-60	24	16

Figure 2. RALS Geometry.

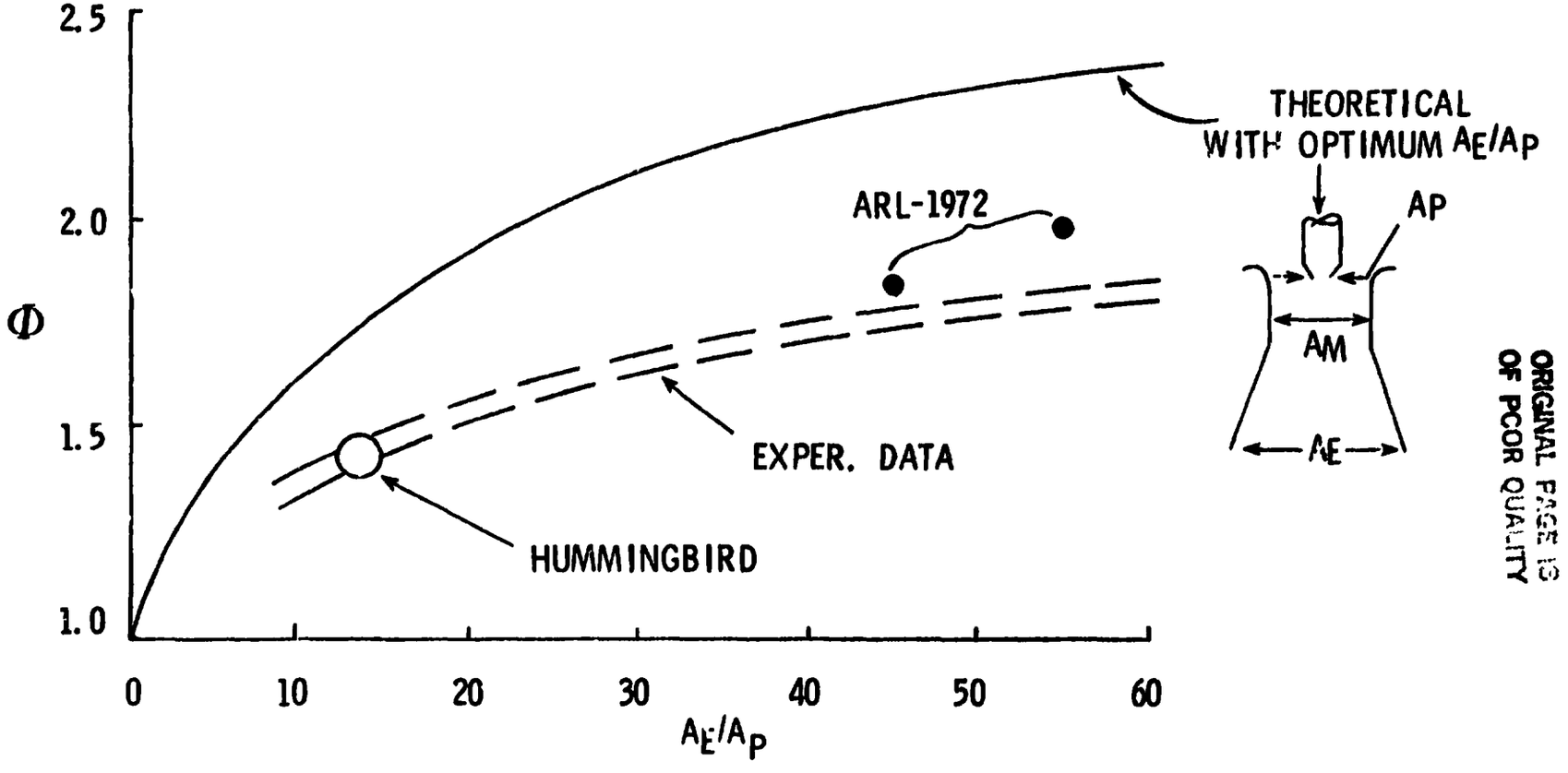

Figure 3. Typical Ejector Augmentation Ratio (Φ).

Augmentation ratio, Φ, is a measure of pumping capability and is usually plotted as a function of area ratio, A_E/A_P. Note that, to achieve augmentation ratios in excess of 1.5, area ratios in excess of 10:1 are required. Area ratios of this magnitude are probably impractical in the space allocated. The categories chosen for the study were as follows:

- Area Ratios 1.0 - 1.1
  - No significant thrust augmentation
  - Provides cooling only
  - Readily vectored
- Area Ratios 1.1 - 1.5
  - Sufficient augmentation to offset weight
  - Vectorable in two planes
- Area Ratios 1.5 - 2.0
  - Significant thrust augmentation
  - Longitudinal vectoring only
- Area Ratios 10 - 20
  - High augmentation levels
  - Nonvectorable
  - Burner may not be required.

These categories are summarized in Table II.

The decision to utilize the Ames VEO model geometry to determine RALS design requirements delayed this study for several months while the reconfiguration of the VEO design was completed. It also placed certain constraints on the RALS design. For example, the VEO model simulates an aircraft in which the engines are nacelle mounted. The specific planform therefore has a relatively narrow fuselage, and the use of two side-by-side remote nozzles is inappropriate. In an aircraft of this type, the ducts would be tied together to feed a common remote augmentor and nozzle.

3.2 CONCEPT EVALUATION

As described in the requirements section of this report, four categories of ejectors to be used with the RALS system were identified. Sixteen conceptual configurations were selected to evaluate the potential merits of each of these categories. These concepts were sized and sketches were made to illustrate how they could be incorporated in a typical twin engine V/STOL aircraft.

Table II. Ejector Nozzle Categories.

Category	Bay Cooling	Thrust Augmentation ϕ	Burner	Area Ratio A_E/A_P
1	Yes	1.0	Yes	1.0 - 1.1
2	Yes	1.01 - 1.02	Yes	1.1 - 1.5
3	Yes	1.1 - 1.2	Yes	1.5 - 2.0
4	Yes	1.5 - 2.0	?	10 - 20

3.2.1 Configurations Studied

Ejector system sizing criteria were obtained from existing ejector test data (References 5 through 8). These data provide the relationship of inlet area (A_I), secondary area (A_S), ejector throat area (A_M), and exit area (A_E) to the nozzle primary area (A_P) as shown in Figure 4. This sketch is typical of a single RALS nozzle installation. In an installatin where two RALS nozzles are used side-by-side (one burner per engine), the area relationships are to be duplicated on either side of the aircraft centerline.

Figures 5 through 8 show the Category 1 ejector installations where the ejector airflow level is aimed at cooling the RALS bay only. The aircraft mold lines, the engine location, and RALS burner locatin were selected by the aircraft manufacturer. The RALS nozzles, Figures 5, 6, and 7, are capable of deflecting the thrust 15° forward to 30° aft and also 15° to either side of the centerline. Small inlet doors on the fuselage admit bay cooling air. The lower section of the fuselage, at the plane of the RALS nozzles, is sized to provide the required ejector throat area (A_M). Two bomb bay doors are hinged to tne lower, outer edges of the bay and are actuated independently to maintain the desired ejector exit area at all side deflection angles of the RALS nozzle.

Configuration 1A, shown in Figure 5, utilizes inlet doors in the top of the aircraft fuselage. The doors are hinged near the aircraic axial centerline to permit the ejector cooling air to flow easily between the RALS burners as well as over their outside surfaces adjacent to the aircraft structure. Flow between the burners is beneficial to the hydraulic actuation components which provide the vectoring and nozzle area variation functions.

Configuration 1B, shown in Figure 6, is the same as Configuration 1A except that the inlet doors are located on the sides of the fuselage. This design would favor the aircraft structure and provide less cooling air to the area between the burners.

Configuration 1D is shown in Figure 7 and utilizes a single RALS burner fed from the two engines. It is otherwise the same as Configuration 1B. This design offers the installation advantage of smaller overall width of the burner since the diameter of the burner is $\sqrt{2}$-D as compared to 2-D for side-by-side nozzles of the same flow area. Cooling air distribution is also somewhat simplified with the single burner configuration.

Configuration 1C, shown in Figure 8, utilizes top-mounted doors and two, two-dimensional RALAD nozzles. The rotating two-dimensional bonnet increases the nozzle aft deflection angle from 30° aft to 70° aft of vertical at the expense of side vectoring capacity.

Figure 9 shows a single RALS burner installation sized to obtain an augmentation ratio of about 1.01 as required for the Category 2 studies. This configuration, designated 2A, utilizes larger ejector inlet (A_I) and exit

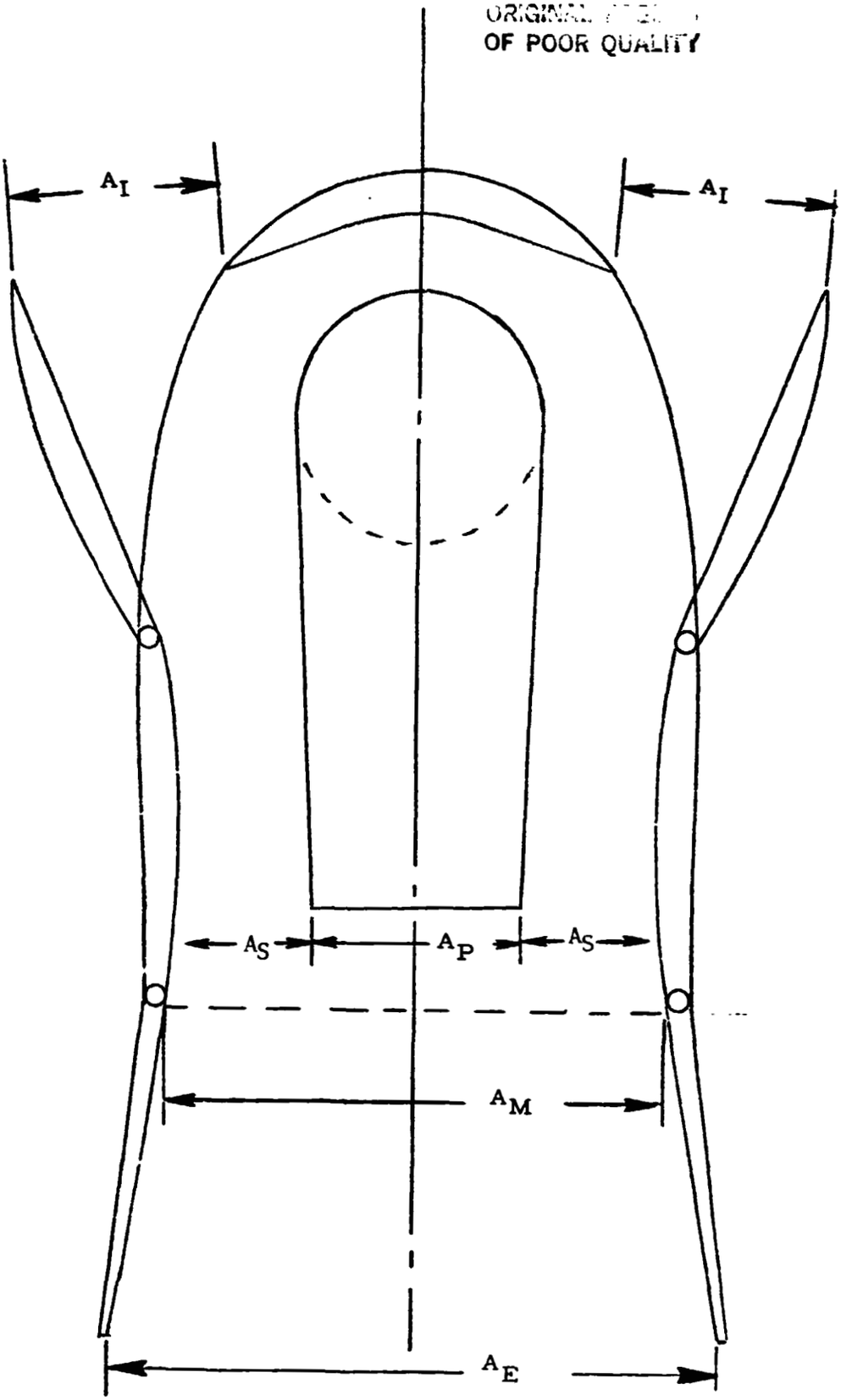

Figure 4. Ejector Schematic.

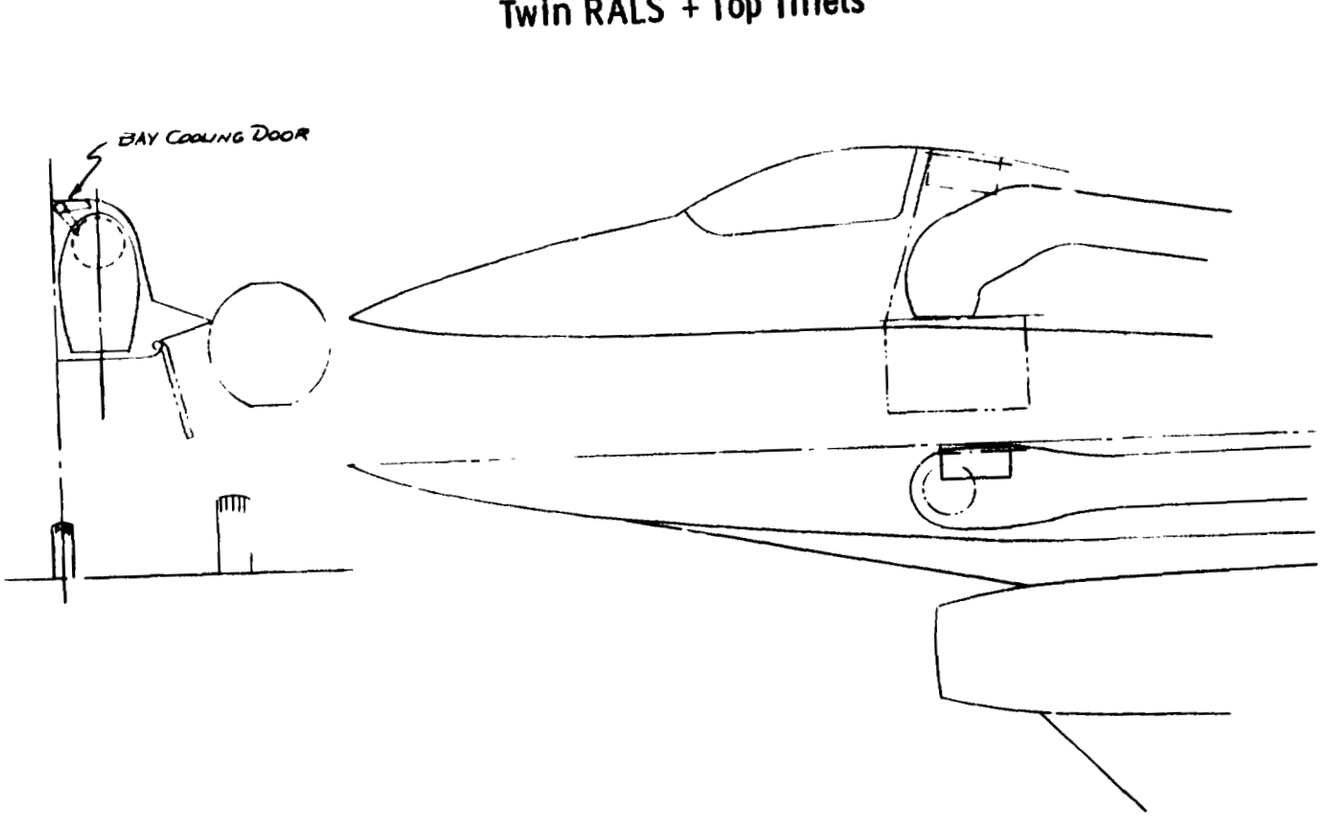

Figure 5. ERALS Category 1 - Design A.

Twin RALS + Side Inlets

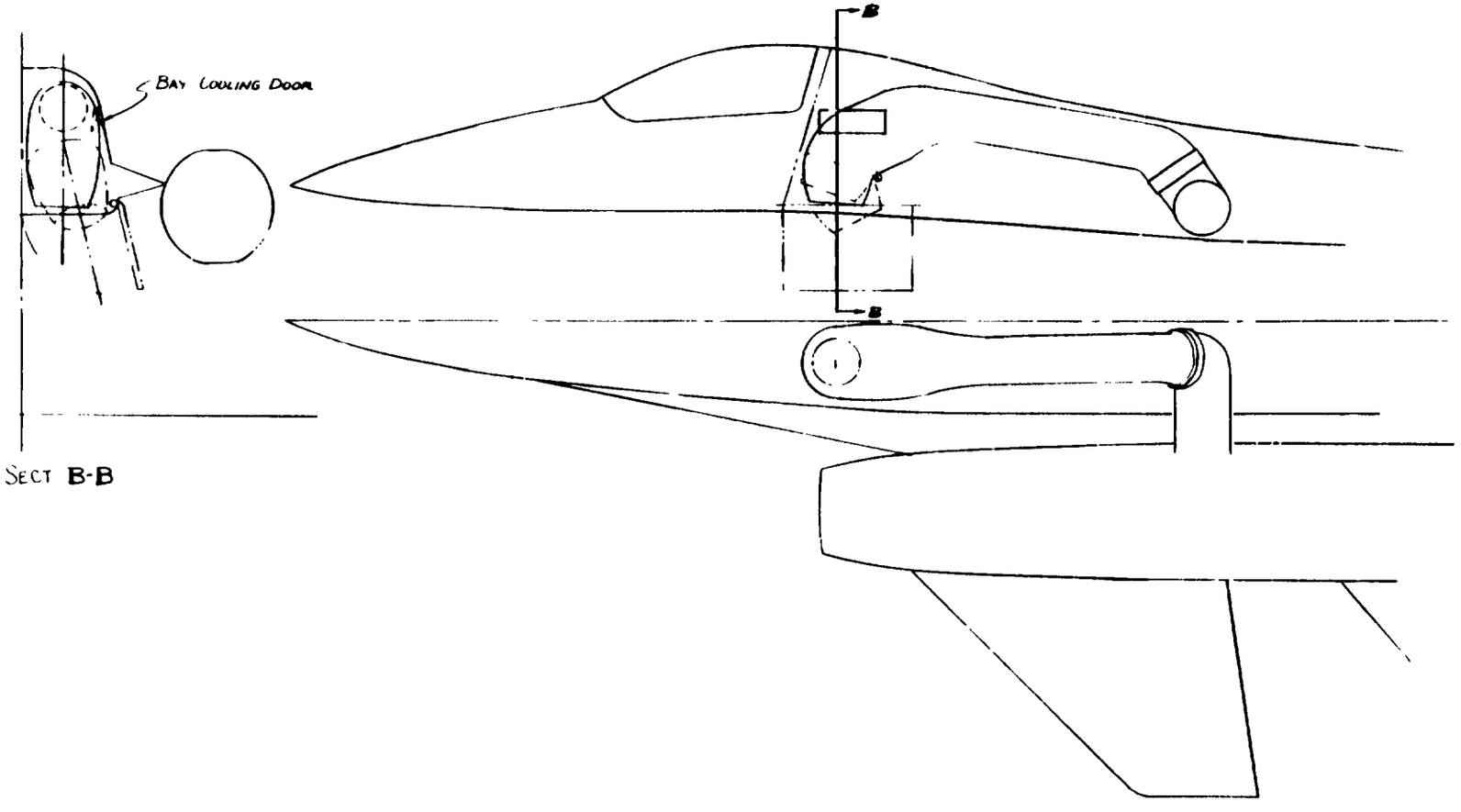

Figure 6. ERALS Category 1 - Design B.

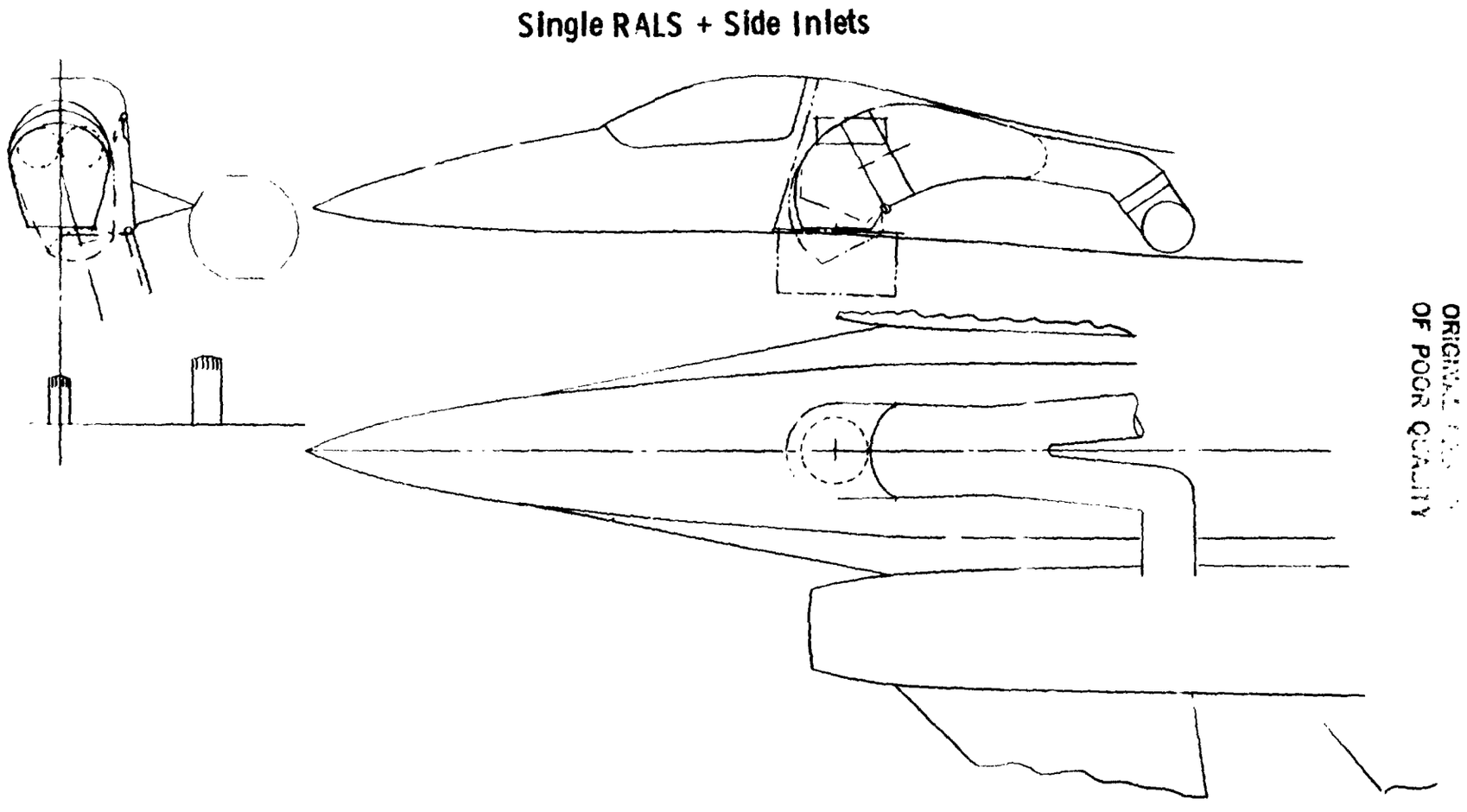

Figure 7. ERALS Category 1 - Design D.

Twin RALAD + Top Inlets

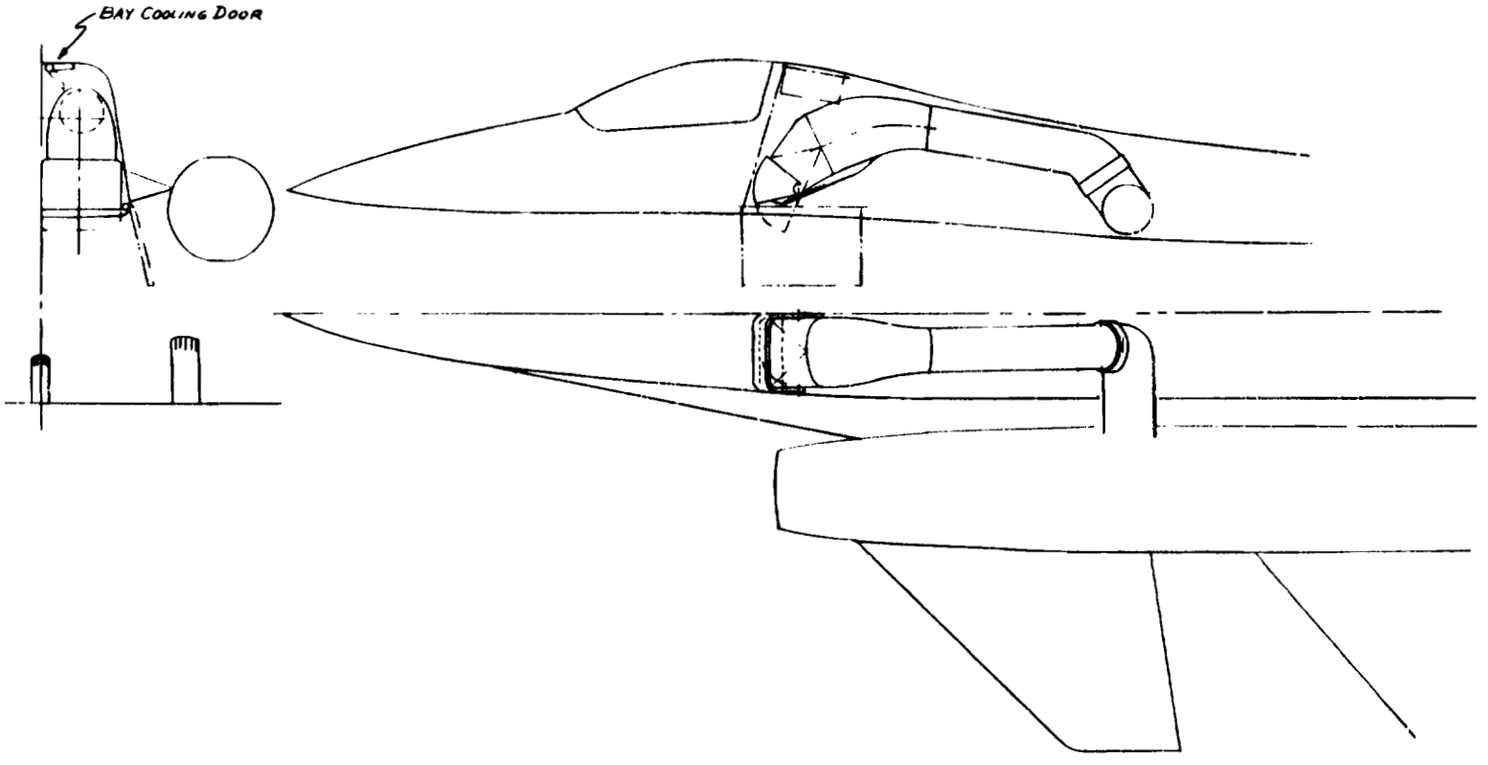

Figure 8. ERALS Category 1 - Design C.

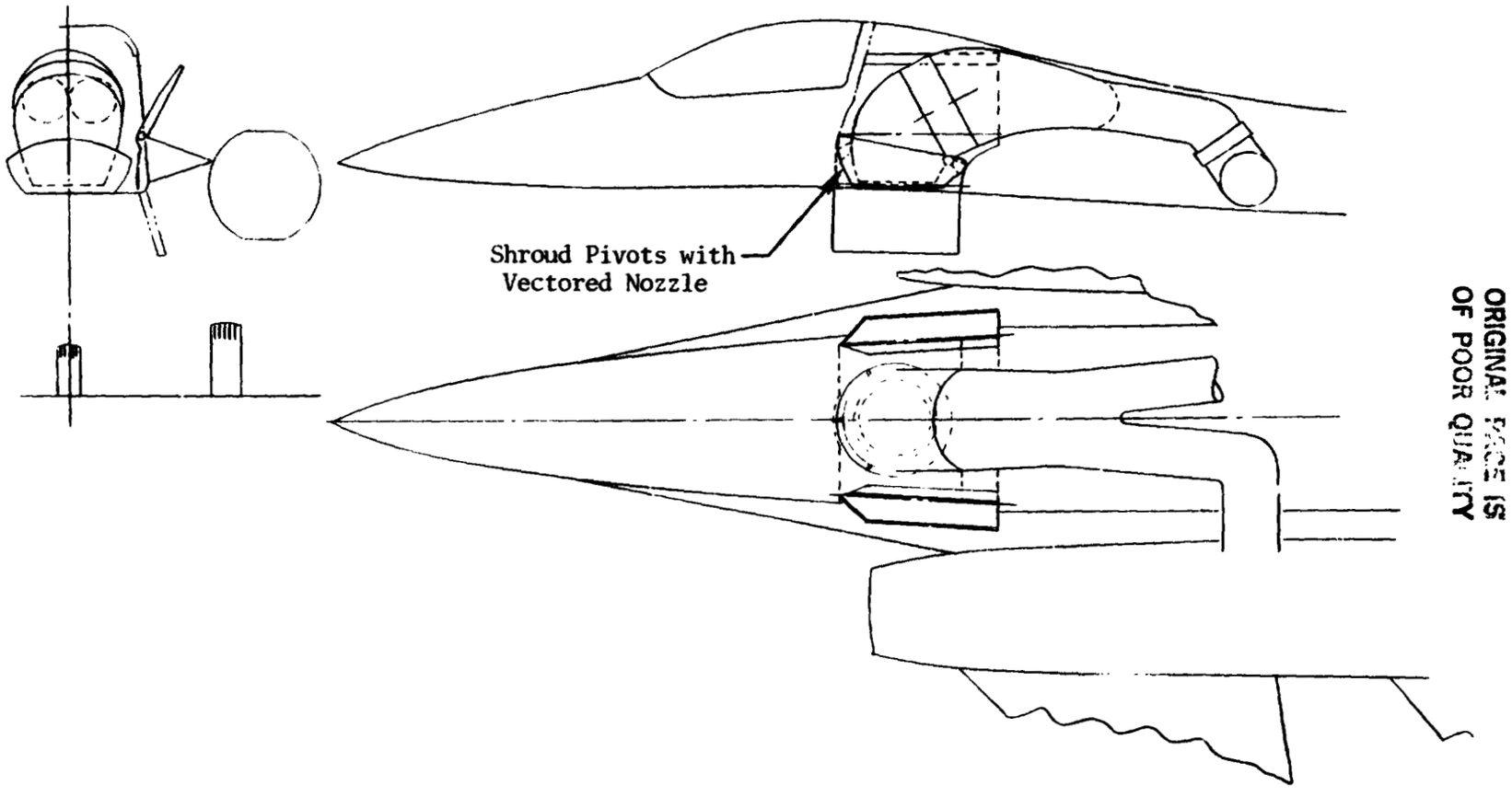

Figure 9. ERALS Category 2 - Design A.

areas (A_E) while the ejector throat area (A_M) is smaller. The smaller ejector throat area-ratio is obtained by attaching a conical shroud to the RALS nozzle. With this arrangement, the ejector throat area/primary throat area ratio, (A_M/A_P) remains constant at all RALS nozzle discharge angles, that is -15° to +30° in the forward and aft direction and ±15° in the side directions. The ejector shroud moves with the primary nozzle during vectoring. The exit doors are actuated independently so the desired exit area can be maintained when the RALS nozzle is vectored to produce side thrust. Similar ejector shrouds and increased inlet area designs were configured for the dual RALS (Configuration 1A) and RALAD (Configuration 1C) designs. The shrouded RALAD design is designated 2C and is shown in Figure 10. In this case, the fore and aft vanes pivot for vectoring and with fixed sidewalls form the ejector shroud. The shrouded dual RALS design is designated 2E and is shown in Figure 11. This shroud is detractable and pivots with the nozzle during vectoring. Configuration 2F which is shown in Figure 12 is similar to the shrouded RALAD design shown in Figure 10 except that small doors have been added to selectively block the ejector flow near the exit plane of the RALAD nozzles. The asymmetry introduced is intended to create low pressure regions to induce a shift in the effective thrust vector angle of the mixed efflux to achieve some level of side vectoring capability. In Configuration 2B, shown in Figure 13, the fixed ejector shroud is replaced by a variable area translating shroud similar to the early General Electric J79 ejector exhaust nozzles. The shroud translation is also used to actuate the variable Ap nozzle. The shroud is fully extended and has its maximum exit area at the full reheat Ap and is fully retracted for stowing at the dry minimum Ap condition.

Configuration 2D shown in Figure 14 employs transverse augmentors close coupled with the engine bleed ports. The augmented flow is then turned downward by curved ducts and forward between articulated doors which set the variable discharge throat area. The forward flowing jet is then deflected downward by a set of three doors at the appropriate lift location. This system occupies the least amount of aircraft volume of all the configurations studied.

Figure 15 shows a configuration which is similar to the Category 1C and 2C RALAD designs which has been modified to satisfy the augmentation ratio goal (1.10 to 1.15) of Category 3. This installation includes two side-by-side rectangular (2-D) burners and RALAD nozzle assemblies. The nozzle aspect ratio was increased to about 5 and it vectors -15° to +30° in the fore and aft plane. Because of the higher augmentation ratio, the ejector inlet area ratio is higher than in the previously discussed nozzles requiring the use of both side- and top-mounted inlet doors. The ejector throat area/RALAD nozzle area ratio is obtained by surrounding the RALAD nozzles with rectangular shrouds. The ejector exit area is obtained by actuating two axially-hinged exit doors. By actuating these exit doors independently, some side force for yaw control can be obtained.

The four other configurations studied in Category 3 were all aimed at increasing the periphery between the RALS nozzle flow and the ejector flow for increased ejector pumping. Configuration 3B which is shown in Figure 16

Twin RALADS + Shroud & Side Inlets

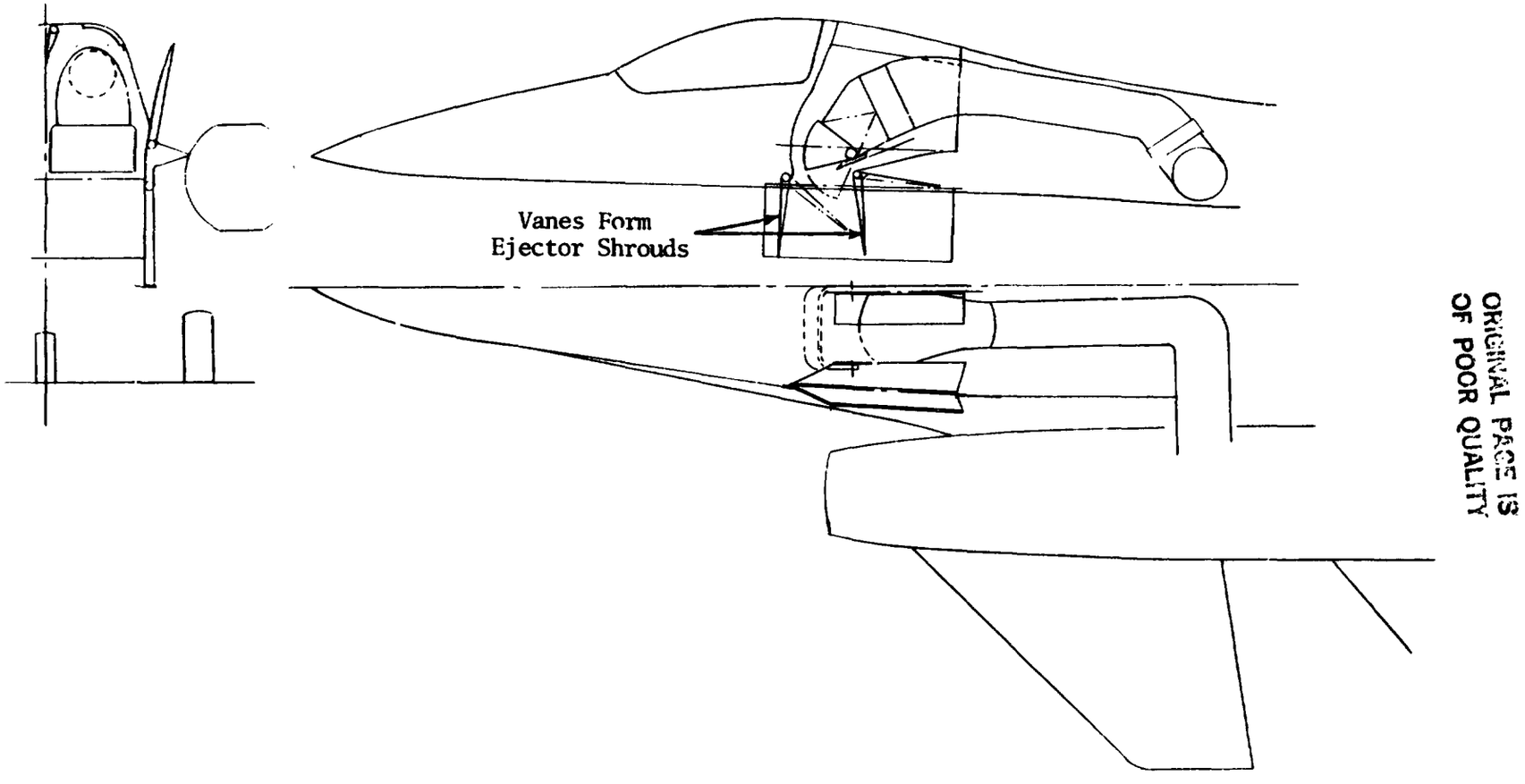

Figure 10. ERALS Category 2 - Design C.

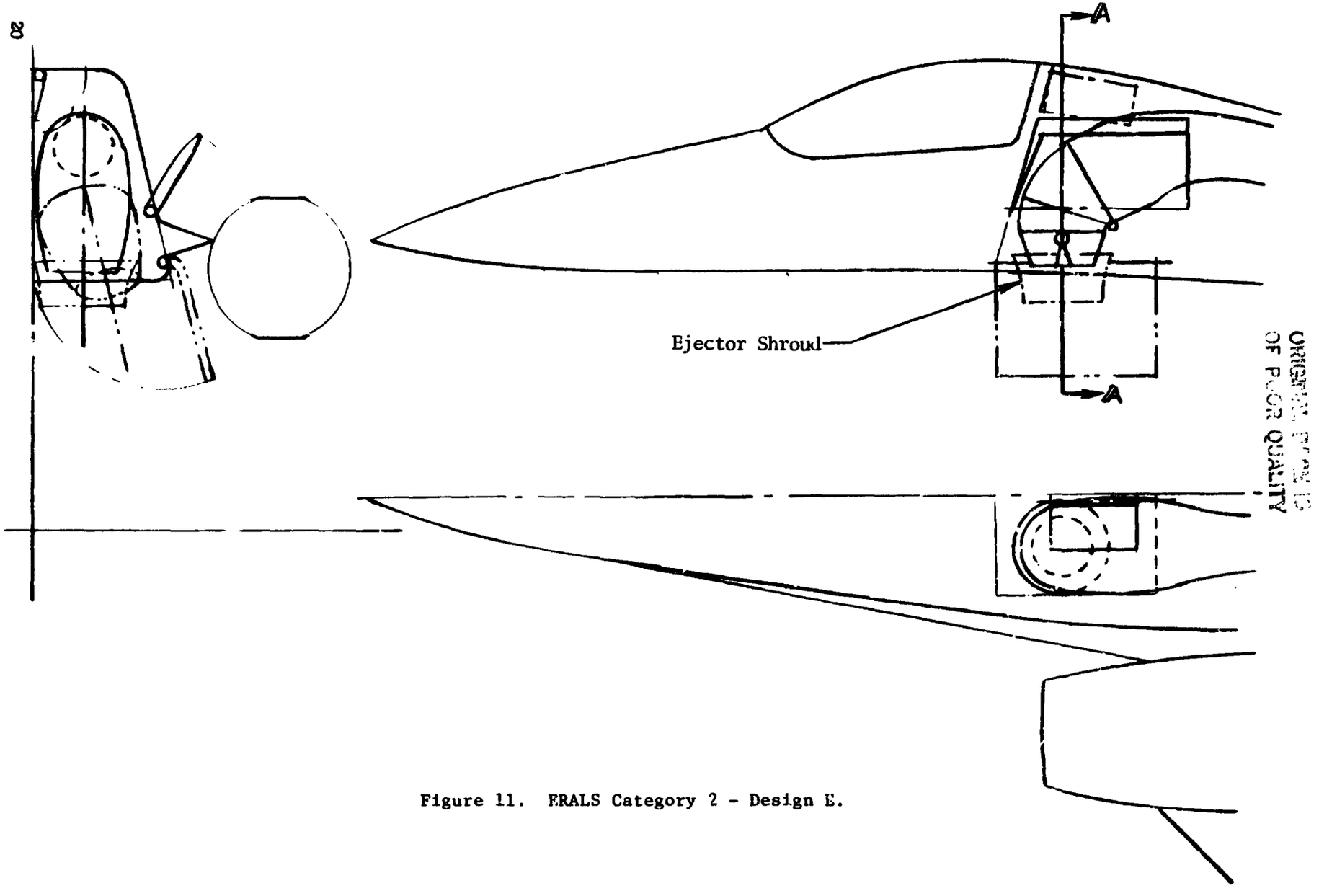

Figure 11. ERALS Category 2 - Design E.

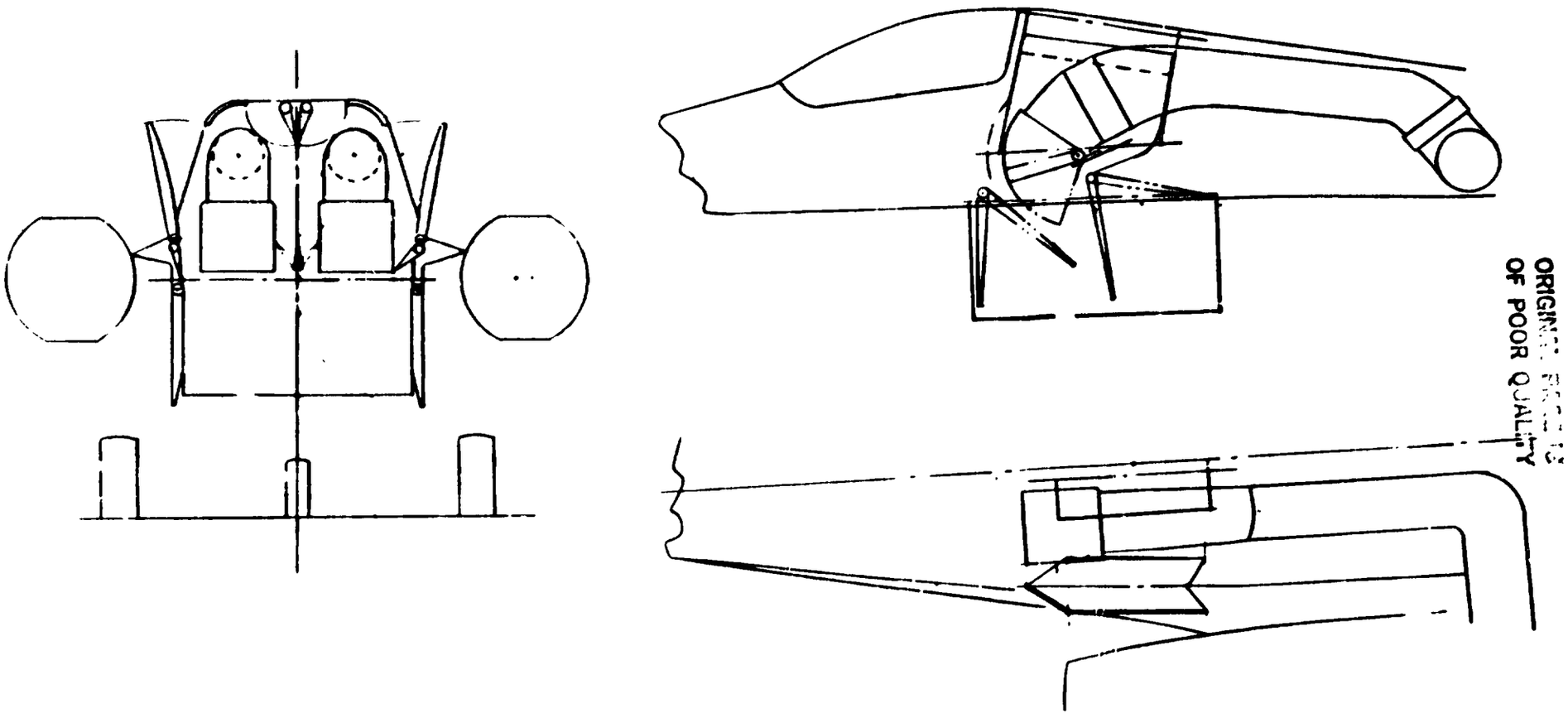

Figure 12. RALAD Plus Shroud and Fluidic Side Vectoring - 2F.

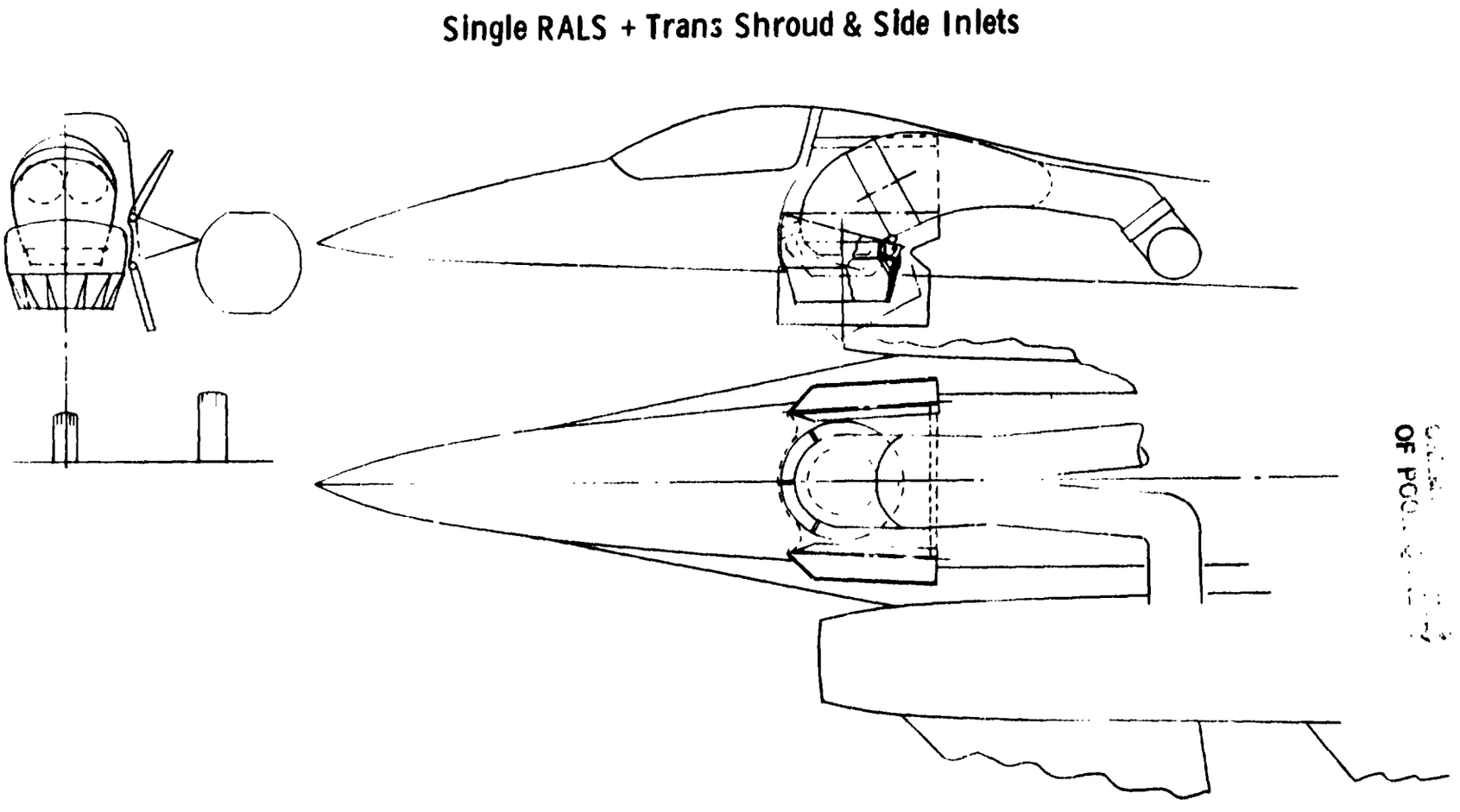

Figure 13. ERALS Category 2 - Design B.

Open Duct

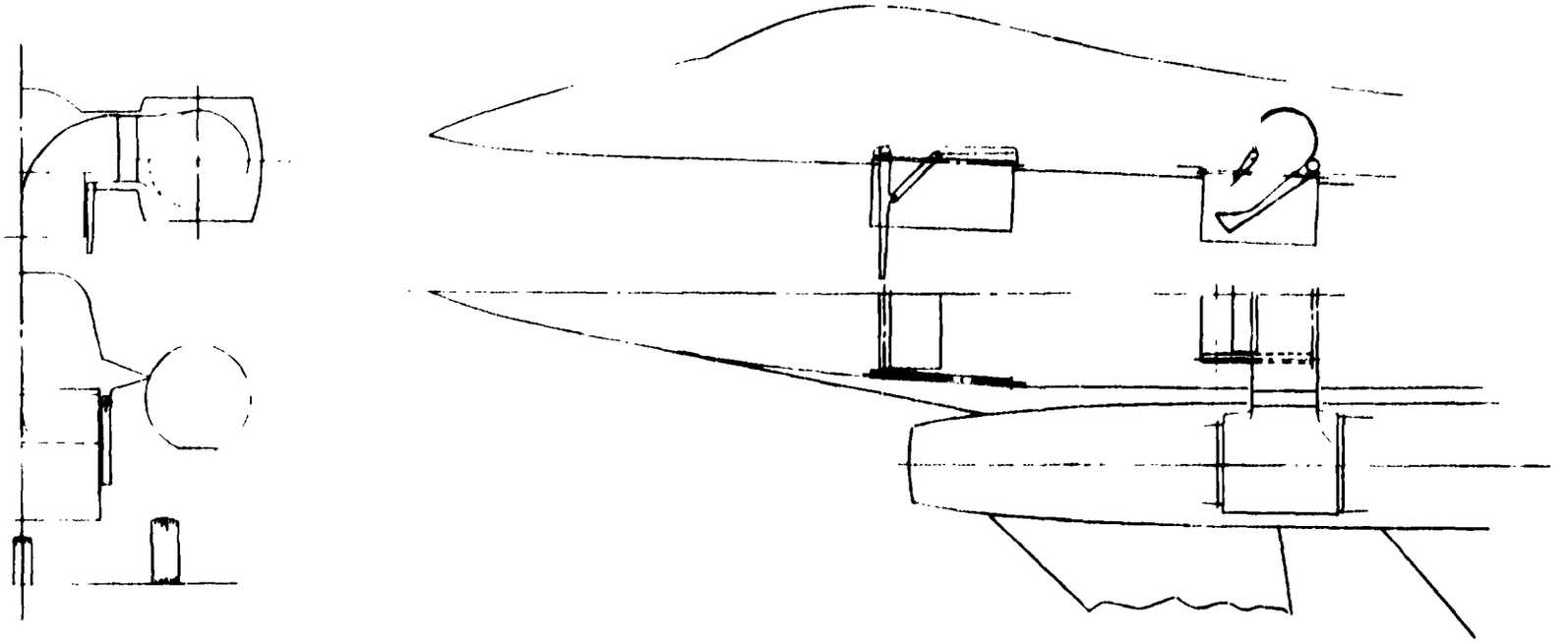

Figure 14. ERALS Category 2 - Design D.

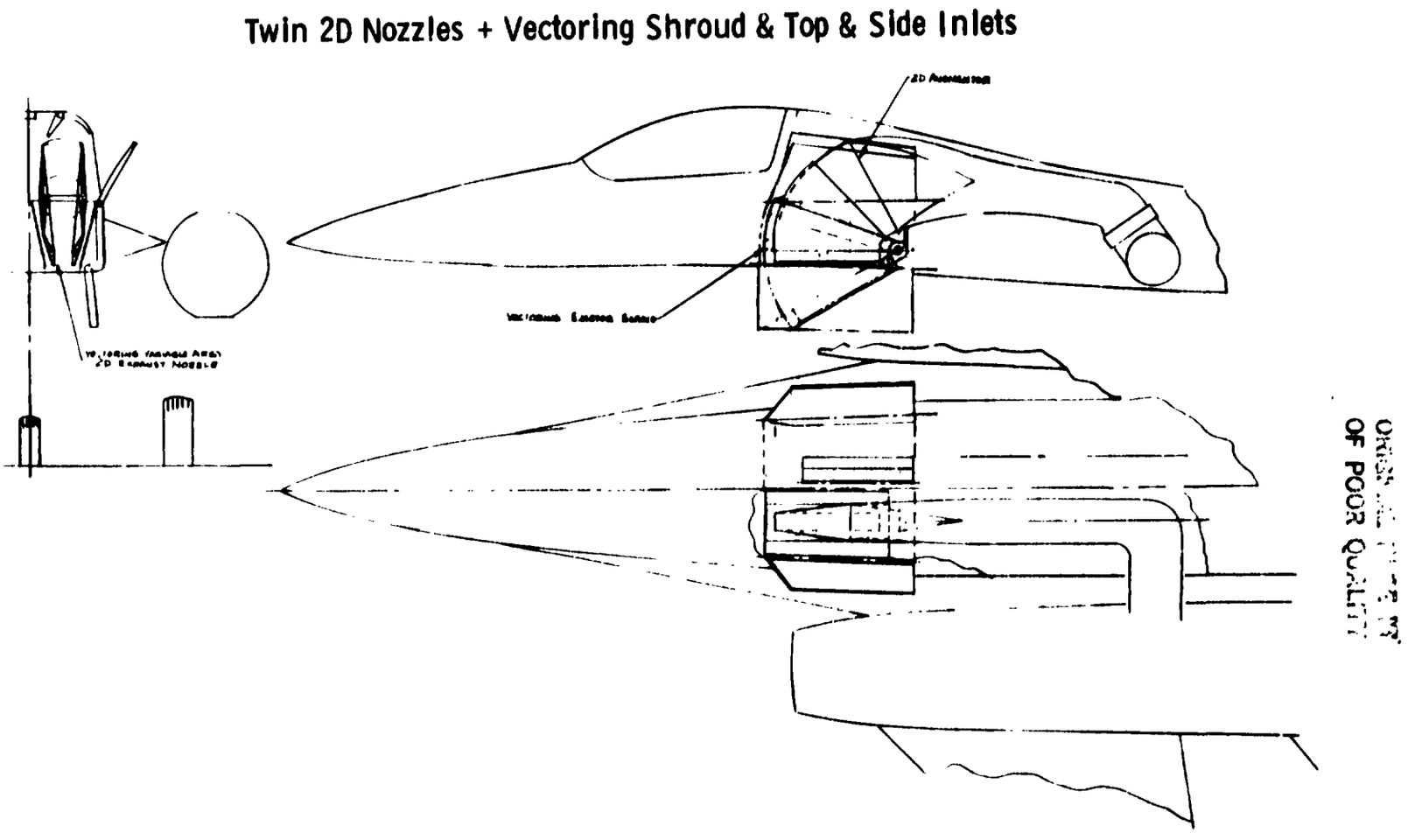

Figure 15. ERALS Category 3 - Design A.

Convoluted 2D Nozzles + Vectoring Shroud & Top & Side Inlets

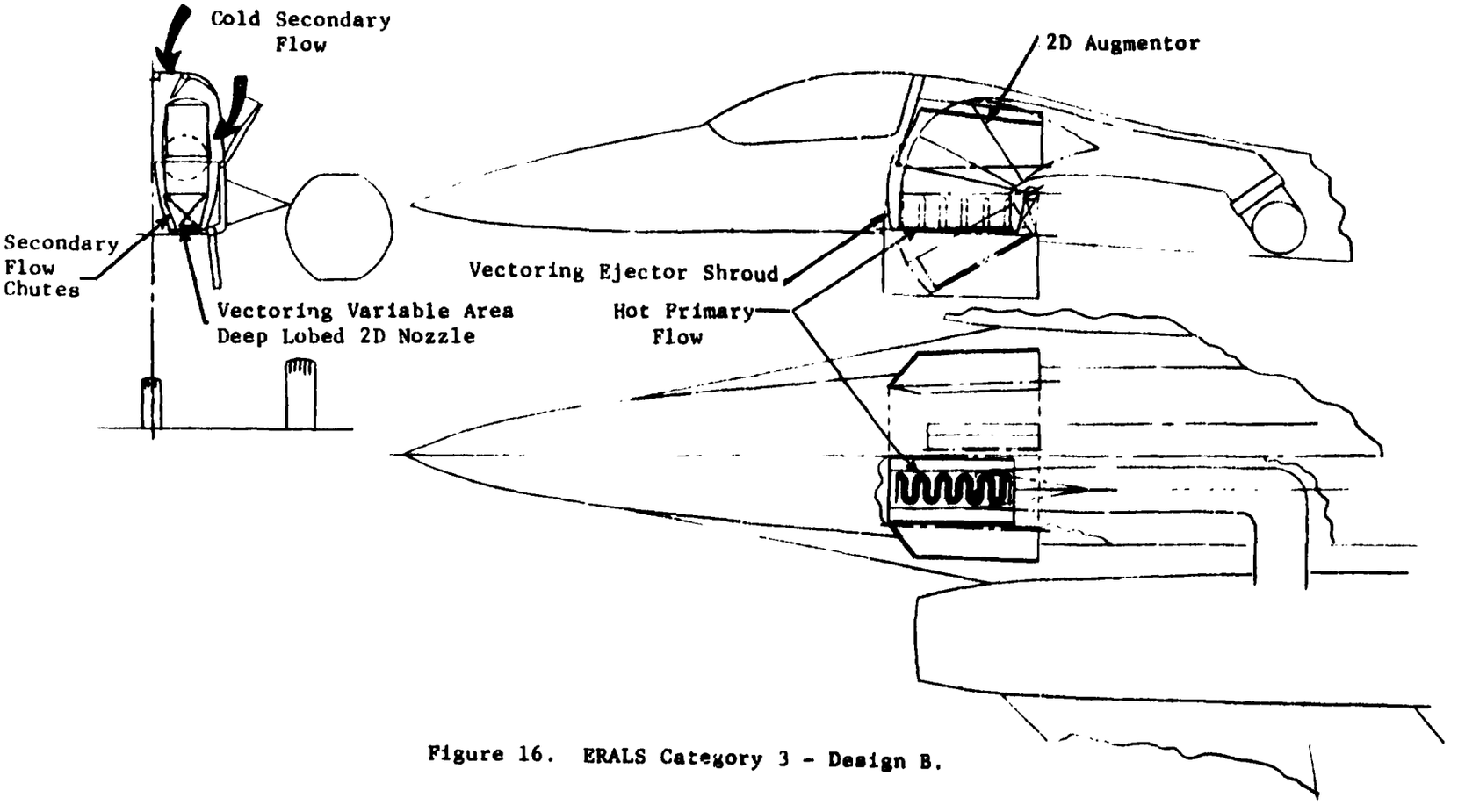

Figure 16. ERALS Category 3 - Design B.

is similar to Configuration 3A except that the nozzle flaps have been deeply corrugated. The flap lobes are indexed to form a long serpentine throat configuration. Each of the flap lobes is open to form an ejector chute for the secondary air.

Configuration 3C shown in Figure 17 employs a deep lobed folding seal star nozzle for the primary variable area nozzle with an ejector shroud.

Configurations 3D and 3E shown in Figures 18 and 19, respectively, are three-stream coannular designs with the augmented primary flow in an annular layer with ejected flow down the center, and also in the outer annulus. Design 3D employs a deep lobed translating daisy nozzle on the inner flowpath between the central ejected stream and the primary flow. Translation of the daisy nozzle provides the nozzle area variation for the reheat primary stream.

In the Category 3E design shown in Figure 19, the inner duct, which contains the central ejected stream, terminates in seven tubes which are completely surrounded by the RALS flow. The second concentric duct, which contains the RALS flow, terminates in a variable area flap and seal nozzle. The outer duct is fixed in geometry. Fore and aft vectoring is accomplished for both the Category 3D and 3E nozzles by differential actuation of the forward and aft transverse cover doors.

A dry high ratio ejector configuration configured for Category 4 is shown in Figure 20. Fan bleed air is simply ducted to high aspect ratio slots in fuselage and canard to satisfy the 30:1 area ratio objective. The number of ejectors/elements would undoubtedly need to be increased and their spacing decreased from the particular configuration shown for adequate ejector performance.

3.2.2 Evaluation

Table III summarizes the basic design parameters including the idealized ejector ratio for the 16 initial configurations. This ideal ratio was computed using a design analysis developed by P.R. Payne (Reference 5). In general, Payne provides a series of charts to evaluate the performance and geometric characteristics of design point ejectors. Thus, beginning with known values of inlet-to-jet area ratio and flow properties, the velocity ratio V_I/V_P was calculated for assumed values of entrainment ratio, N (Figures 21 and 22). By further assuming a diffuser efficiency (for example, $N_O = 0.9$) a design point ejector entrainment ratio was determined as shown for ERALS Design 1A in Figure 23. These values are compared as the "best possible" augmentation ratios in Table III and exhibit a trend directly opposite to that set up by the augmentation goal values. The opposing trends are due primarily to the fact that augmentation goals and assigned values reflecting a RALS bay cooling requirement for the low end of the spectrum (such as Category 1) and high performance at the upper end (Category 4). In contrast, the best

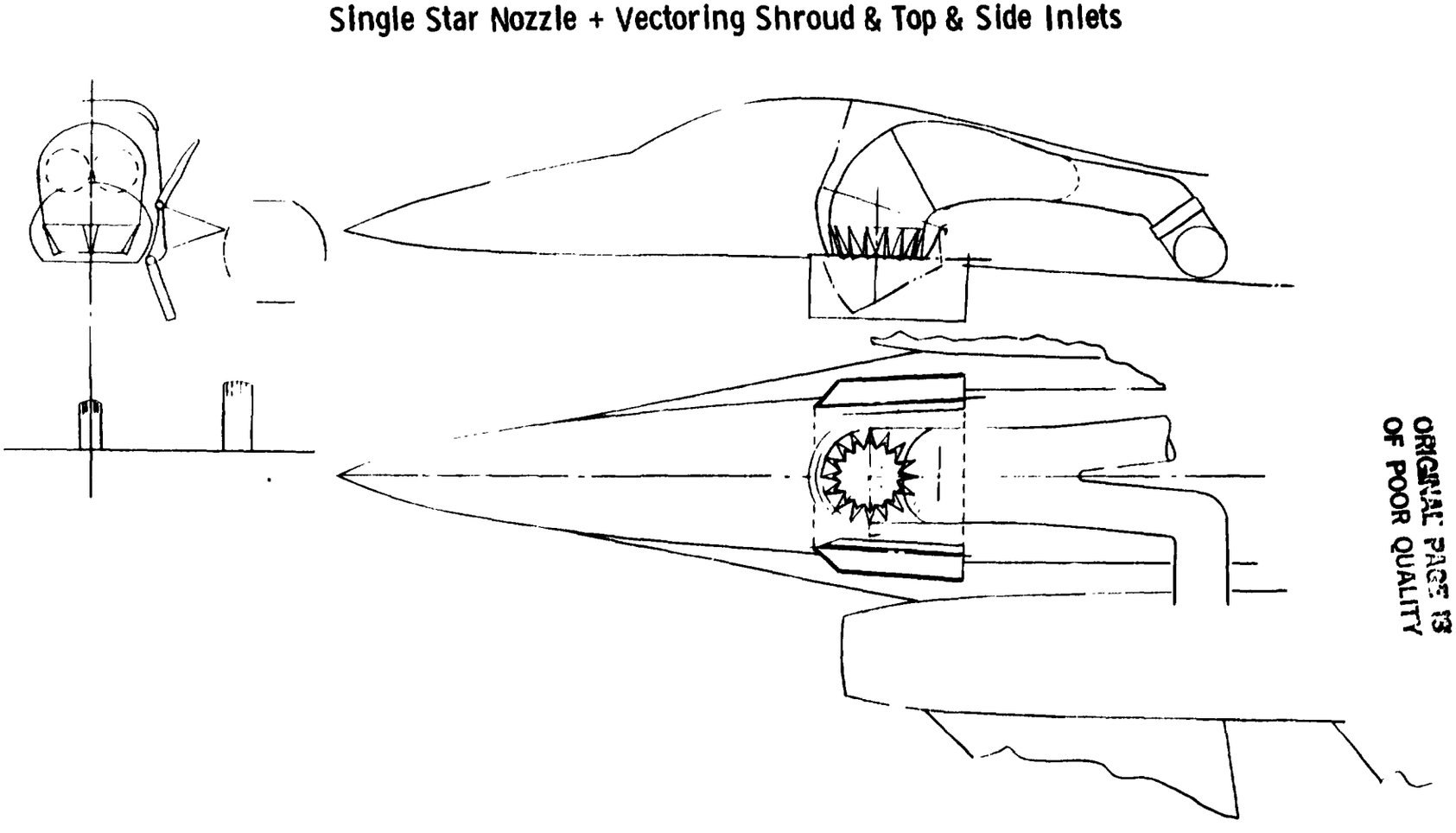

Figure 17. ERALS Category 3 - Design C.

Convoluted Annular Nozzle + Shroud & Top Inlets

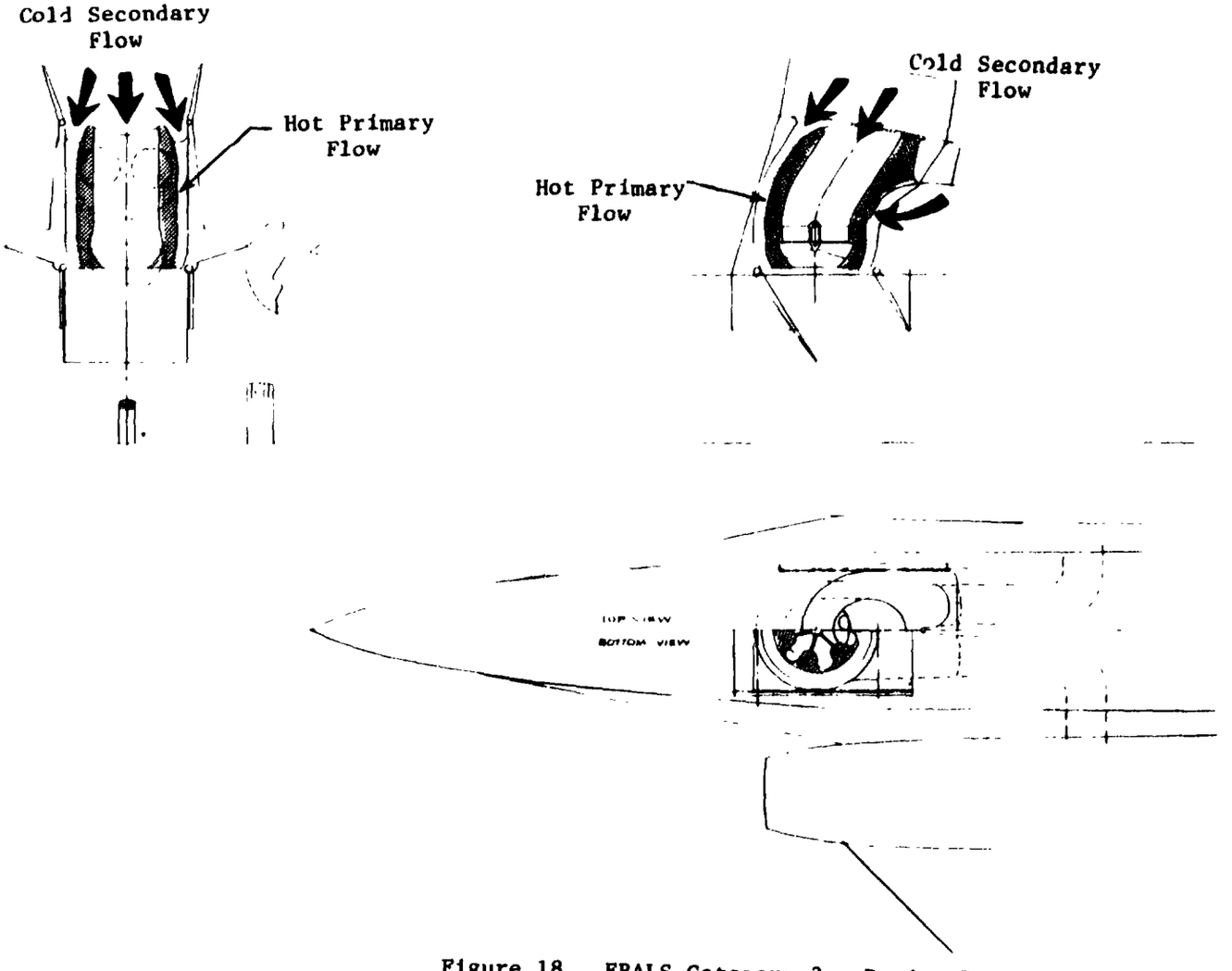

Figure 18. ERALS Category 3 - Design D.

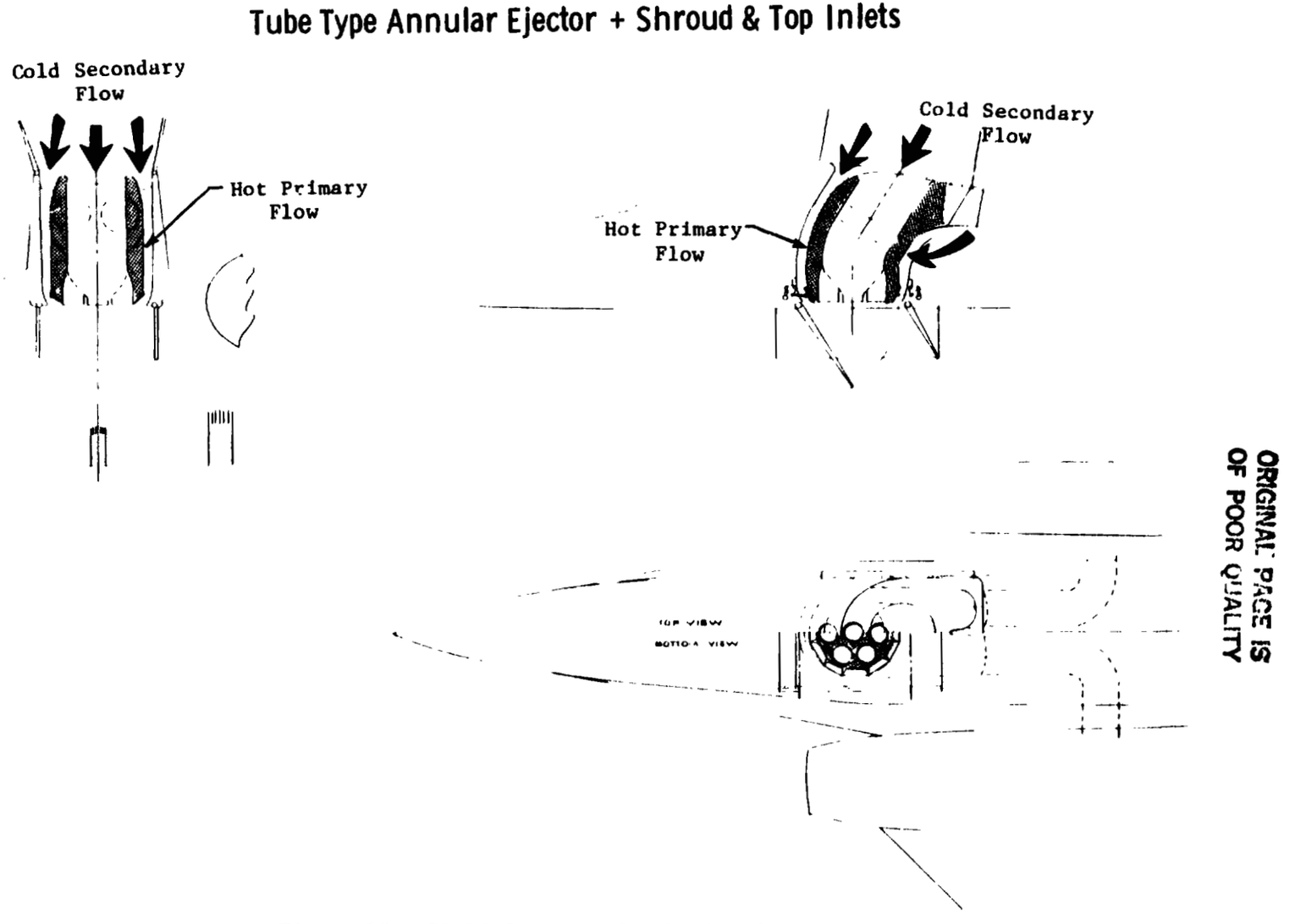

Figure 19. ERALS Category 3 - Design E.

30:1 Area Ratio Ejector

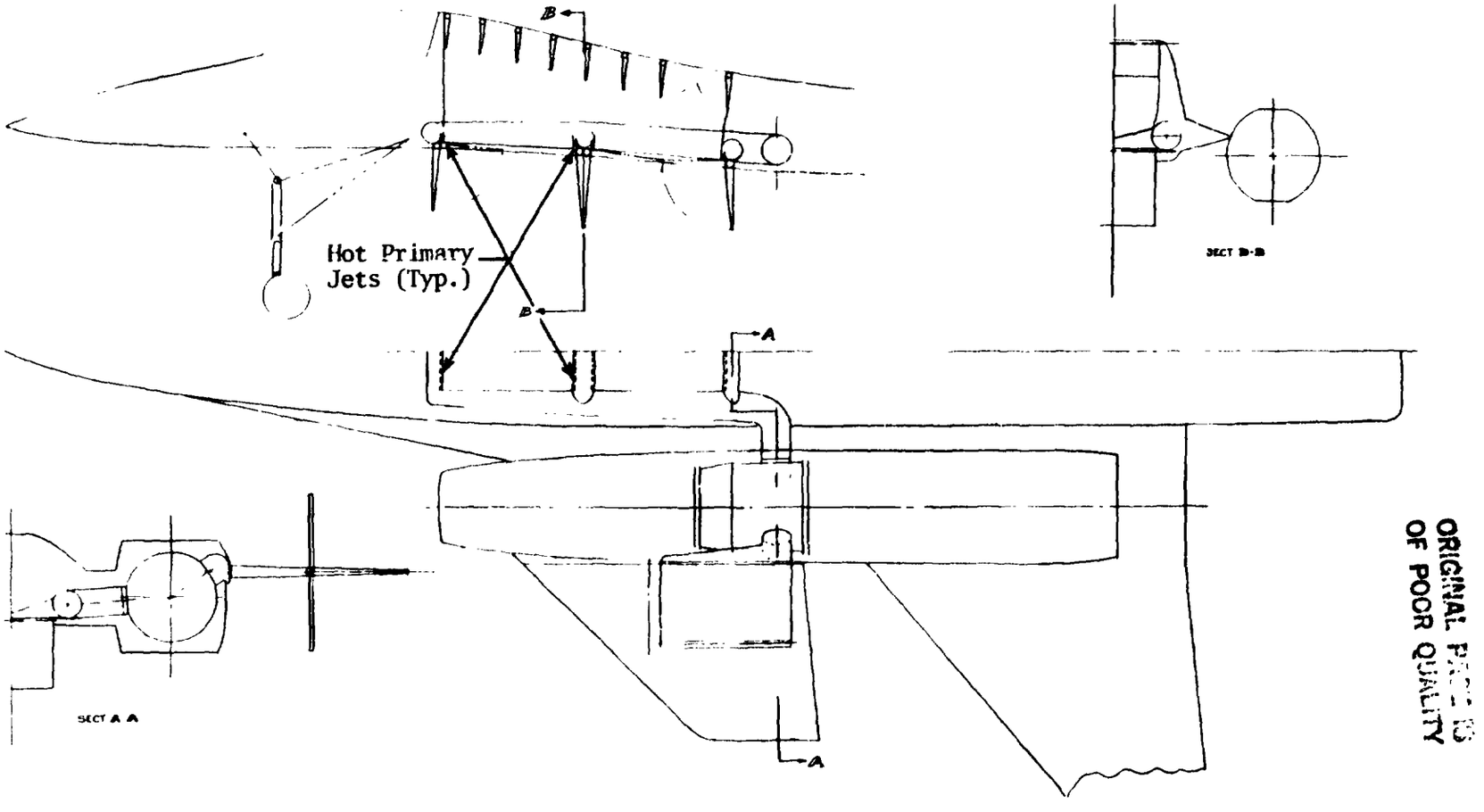

Figure 20. RALS Category 4 - Design A.

Table III. ERALS Configuration Summary.

Cat.	Config.	Description	No. Noz.	A_p/Noz. $in.^2$	A_I/A_p	A_8/A_p	A_8/A_p	Augmentation Ratios - ϕ Goal	Augmentation Ratios - ϕ Best Possible
1	A	Current RALS + Top Inlet	2	200	0.6	5.6	≈7.4	Cooling Only	1.7
1	B	Current RALS + Side Inlet	2	200	0.4	5.6	7.4	Cooling Only	1.7
1	C	RALAD + Top Inlet	2	200	0.6	4.4	7.2	Cooling Only	1.6
1	D	Single Current RALS + Side Inlets	1	400	0.4	4.4	5.6	Cooling Only	1.6
2	A	Single Current RALS + Vectoring Shroud + Side Inlets	1	400	2.5	1.3	5.6	1.01 to 1.02	1.2
2	B	Trans. Vect. Shroud + Side Inlets	1	400	2.5	1.6	7.0	1.01 to 1.02	1.2
2	C	RALAD + Side & Top Inlets	2	200	3	3	3.5	1.01 to 1.02	1.4
2	D	Open Duct	2	200	-	$A_{Deflector}/A8=6.5$		1.01 to 1.02	
2	E	RALS w/Top & Side Inlets + Shroud	2	200	3	1.9	-	1.01 to 1.02	1.2
2	F	RALAD + Vect. Shroud & Fluidic Side Vectoring	2	200	3	3	3.5	1.01 to 1.02	1.4
3	A	Vectoring Variable Area 2-D Nozzle + Shroud	2	200	3.6	2.0	5.0	1.10 to 1.15	1.2
3	B	Vectoring Variable Area Deep Lobed 2-D Nozzle + Ejector Shroud	2	200	4	2.0	5.1	1.10 to 1.15	1.2
3	C	Star Primary + Ejector Shroud	1	400	2.6	2.0	5.7	1.10 to 1.15	1.2
3	D	Annular Corrugated Truncated Plug	1	400	5	2.0	5	1.10 to 1.15	1.2
3	E	Annular Truncated Plug + Tubes	1	400	5	2.0	5	1.10 to 1.15	1.2
4	A	XV12A Type	1	400			30 to 60	2.0 to 2.10	

Symbols defined in Figure 4

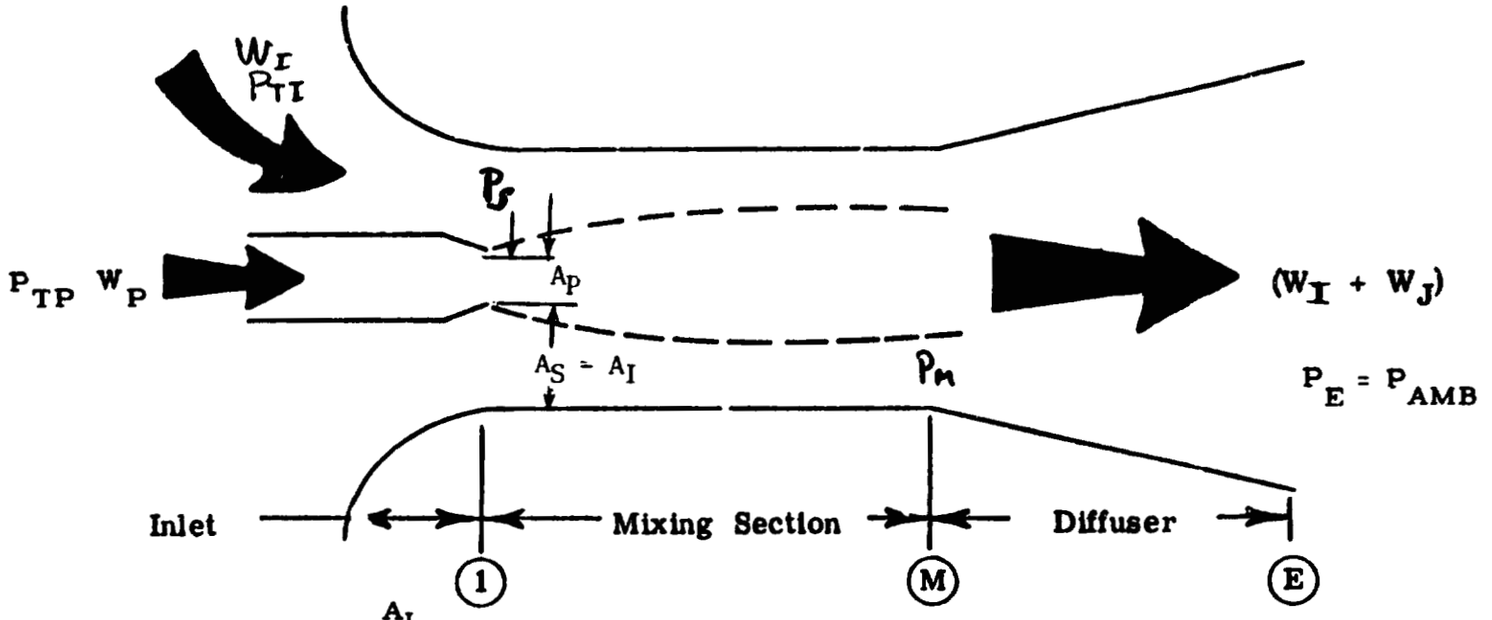

$\frac{A_I}{A_P}$ - SECONDARY-TO-JET AREA RATIO

$\frac{A_E}{A_M}$ - DIFFUSER AREA RATIO

$\frac{W_I}{W_P}$ - SECONDARY-TO-JET WEIGHT FLOW RATIO

$\frac{P_{TP}}{P_a}$ - JET PRESSURE RATIO

Φ_{IE} - IDEALIZED EJECTOR AUGMENTATION RATIO
- MIXED FLOW GROSS THRUST/PRIMARY FLOW GROSS THRUST

Figure 21. Idealized Ejector.

DEFINE $N = \frac{W_I}{W_P} = \frac{\rho_I A_I V_I}{\rho_P A_P V_P}$

CALCULATE $\frac{V_I}{V_P} = K \frac{P_P}{P_I} \frac{T_I}{T_P} \left(\frac{1}{\frac{A_M}{A_P} - 1} \right) N = f \left(\frac{A_M}{A_P}, N \right)$

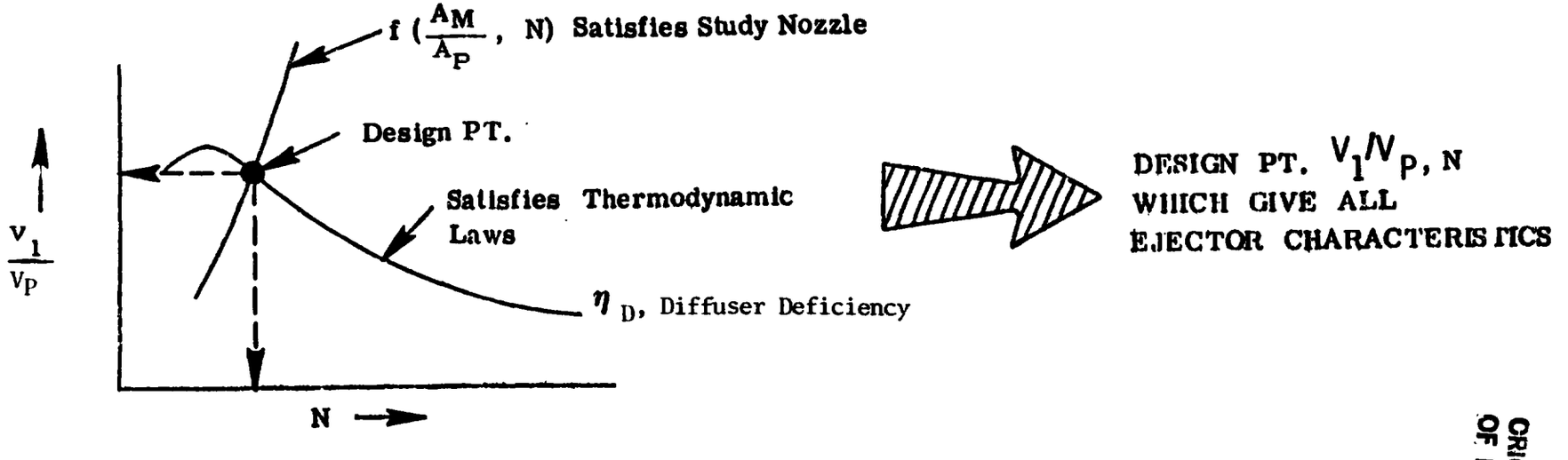

Figure 22. Performance Estimate-Idealized Ejector.

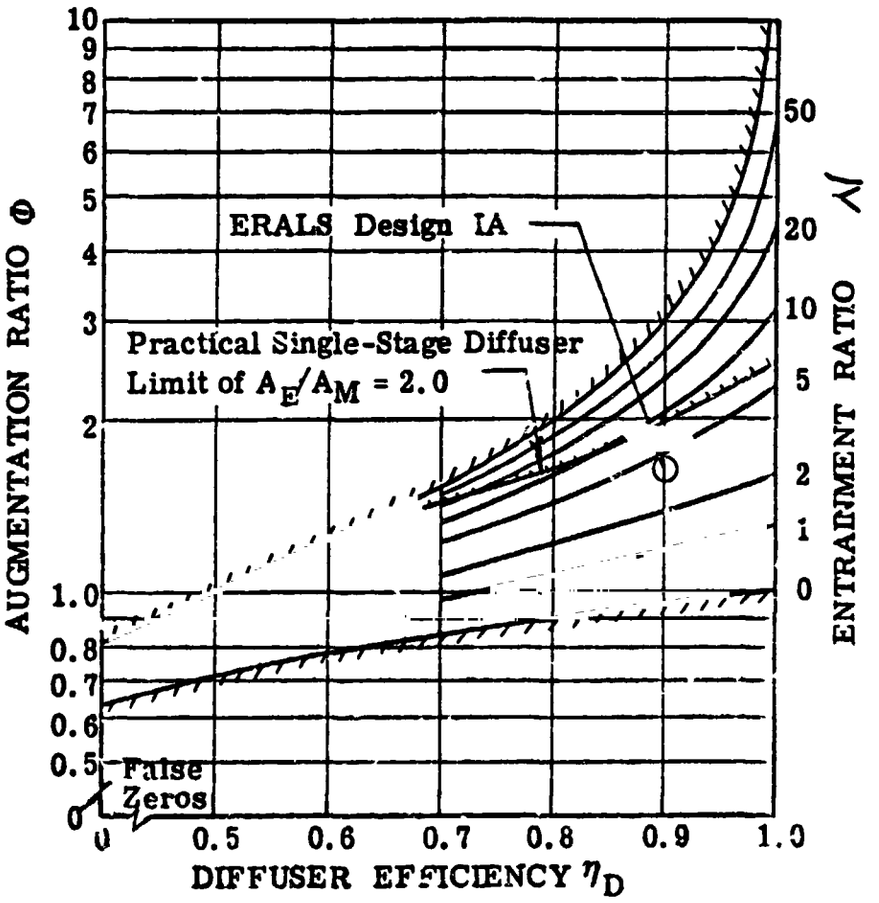

Figure 13. Idealized ERALS Performance.

possible augmentation ratios were determined from installed geometry area ratios and, therefore, produce the more realistic trend. Earlier exit-to-primary area ratios corresponding to the augmentation goals were also similarly developed and have generally lower values (A_E/A_P in Table II) compared to the higher values calculated for installed geometries as listed in Table III. In general, the actual design flowpath departs from the ideal shape necessary for realizing the best possible augmentation ratio. Therefore, derates were established to account for nonideal ejector losses and to arrive at more realistic performance values. However, an accurate estimate of these losses could only be obtained by either more extensive analytic evaluation or by testing of detailed models.

Since data from such sources were lacking, the performance derates were determined subjectively. The general approach was to visually note geometric variations from an ideal ejector flowpath and to then consider feasible design improvements. The finalized relative augmentation ratios shown in Table IV were calculated by using Design 1A augmentation ratio as a base value. Relative values of 1.00, therefore, represent an actual value that could be less than or more than unity depending on the design flow losses.

Four other key evaluation factors are shown in Table IV. The estimated weight of each design is given as an incremental weight increase over a conventional RALS system with vectoring capability and without secondary flow. The incremental weight increase, therefore, represents the penalty for adding hardware to provide a secondary flow and enhance ejector performance. The lone exception to this is the open duct design 2D which is not an ejector and has no augmentation capability. The large weight increase represents structural weight required to deflect the reheat jet.

Other parameters of importance are the relative jet height-to-equivalent-diameter ratio and relative jet perimeter. Jet height should be small for reduced ground impingement velocities and reduced aircraft suckdown during VTO operation. Jet perimeter should be large to enhance secondary flow entrainment. Two designs, 3D and 3E, require increased envelopes for containing the flowpath volume. Since the larger envelope results in increased frontal area and higher drag during cruise, it will result in reduced aircraft performance during cruise.

In the study of those concepts falling in Category 1, it was determined that to provide adequate bay cooling internal guide vanes and inlet doors were required. In addition, a shroud is very desirable over the jet to provide a mixing section to ensure a secondary airflow. When these features are added, the geometry can be adjusted to provide some thrust augmentation in all cases. Therefore, the simpler concepts were upgraded from Category 1 to Category 2 and Category 1 was dropped from further consideration.

The one ejector concept identified for Category 4 required a very large secondary-to-primary area ratio to achieve the high augmentation goal. This concept involved an extended two-dimensional throat configuration which, because of Reynold's number and boundary layer effects, would not lend itself

Table IV. ERALS Design and Performance Characteristics Summary.

Configuration	* Weight lb	** Relative Augmentation Ratio Φ	*** Relative Jet Size ip/Dg	Relative Jet Exit Perimeter, in.	Relative Frontal Area in.^{2}	Jet Power Setting	Jet Vector Capability δ - degrees Aft/Fwd/Side	Selected For Task III
A - RALS w/Top Inlets	13.1	1.00	1.00	1.00	1.00	R/H	30/15/15	
B - RALS w/Side Inlets	13.1	1.00	1.00	1.00	1.00	R/H	30/15/15	
C - RALAD w/Top Inlets	301	1.00	0.52	1.29	1.00	R/H	70/15/0	
D - Single RALS w/Side Inlets	26.5	1.00	1.41	0.71	1.00	R/H	30/15/15	
A - Single RALS w/Shroud	101.5	1.08	1.41	0.71	1.00	R/H	30/15/15	
B - Trans. Ejector Shroud	237.5	1.00	1.41	0.71	1.00	R/H	30/15/15	
C - RALAD w/Ejector Shroud	479	1.17	0.52	1.29	1.08	R/H	70/15/0	*
D - Open Duct	678	0.72	-	-	1.00	R/H	0/30/0	
E - RALS w/Top & Side Inlets + Shroud	56	1.17	1.00	1.00	1.00	R/H	30/15/15	*
F - RALAD + Vect. Shroud & Fluidic Side Vectoring	505	1.17	0.52	1.29	1.08	R/H	70/15/5	
A - Hi AR 2D Vector Nozzle	625	1.17	0.33	1.57	1.08	R/H	30/15/0	
B - Deep Lobe 2D Vector Noz.	731	1.17	0.13	3.79	1.08	R/H	30/15/0	
C - Star Primary Nozzle	146.5	1.00	1.38	1.19	1.08	R/H	30/15/15	
D - Conv. Annular Ejector	427	1.00	0.38	2.13	1.24	R/H	30/15/0	
E - 7 Tube Annular Ejector	459	1.17	0.25	2.71	1.24	R/H	30/15/0	*
A - 30:1 Dry Ejector	47.2	1.50	0.06	2.20	0.70	Dry	15/15/15	

* Baseline = RALS for 2 Engines ** Includes design improvement and durate for system losses *** Single Jet Diameter

well to small scale model testing. In addition, the large uncertainty of pumping characteristics of such an ejector raises questions of achieving the desired augmentation ratio. Since this configuration can only operate dry, it is unlikely that it could provide thrust comparable to the augmented systems of Categories 2 and 3. Therefore, the selection of concepts for Task 3 was reduced to consideration of Categories 2 and 3 only.

An important consideration in concept selection is the ability to meet thrust vectoring requirements. These requirements generally fall into two categories:

(1) $\pm 15^{\circ}$ side vectoring for yaw control

(2) 70° aft vectoring for STOL takeoff

Of the nozzles and ejector concepts considered, none meets both requirements. Therefore, in systems designed for STOL capability, some other means for yaw control must be provided, such as bleed jets.

In selecting ejector concepts for further preliminary design analysis, it is desirable that at least one concept have side vectoring capability, and at least one concept have high aft vectoring capability. In addition, one concept may be of interest without regard to vectoring capability, but with maximum thrust augmentation potential. With these objectives, the following concepts were selected for further evaluation in the preliminary design phase of this study:

- RALS nozzle with four inlet doors and shroud (side vectoring), Concept 2E, reference Figure 11
- RALAD nozzle with ejector doors (aft vectoring), Concept 2C, reference Figure 10
- Single seven tube annular ejector with doors, Concept 3E, reference Figure 19.

3.3 ANALYTICAL METHODS

The available literature was surveyed to provide an appropriate methodology for establishing ERALS performance as well as a quantitative basis for concept selection. It was immediately clear that a great deal of analytical and experimental work has already been done for selected groups of configurations. These analyses as well as the test data spanned a broad spectrum of ejector possibilities from simple single-stage configurations to hypermixing multistage devices. Unfortunately, the greater portion of the available results did not satisfy the geometric requirements or flow conditions for the ERALS concepts. However, four selected analytic treatments shown in Table V and References 5 through 8 were judged to be applicable to the present program and in addition produced results supported by varying amounts of test data.

Table V. Ejector Literature Review Representative Summary.

Reference	Authors	Title	W_S/W_P	T_{TP}/T_{TS}	A_M/A_P	A_E/A_M	P_{TP}/P_{AMB}
5. USA AVLABS TR66-18 1966	P.R. Payne	Steady State Thrust Augmentors and Jet Pumps	1→50	1.0	3→20	1.5→4	-
6. NASA CR-1602 1972	K.E Hickman G.B. Gilbert J.N. Carey	Analytical and Experimental Investigation of High Entrainment Jet Pumps	10→40	1.5→8	143→1000	-	7→27
7. AIAA Peper 72-1174 1972	B. Quinn	Recent Developments in Large Area Ratio Thrust Augmentors	-	1.0	20→25	1→2.6	-
8. APL 75-0224 1975	H. Viets	Thrust Augmenting Ejectors	2→5	1→2.7	-	1→2.5	1→7

In particular, Reference 5 was used to conduct concept evaluations outlined in Section 3.2.2. References 6 and 7 were used to determine the performance of the preliminary design as described later. Reference 8 has essentially the same analytical approach as References 5 and 6 but is referenced to document its range of test data.

3.3.1 Ideal Ejector Analysis

The "Ideal Ejector Analysis" is based on a methodology developed by P.R. Payne (Reference 5). Payne assumes an axisymmetric idealized ejector shown schematically in Figure 21. This ejector has three elements: (1) an inlet section made up of an axisymmetric jet flow, W_P, and an annular bellmouth which admits secondary flow, W_S; (2) a mixing section in which the primary and secondary flows go through complete mixing; and (3) a diffuser section which supports a pressure rise from mixed pressure P_M to ambient static, P_{AMB}. The ability of an ejector to pump secondary flow and produce increased thrust (i.e., thrust augmentation, $\phi_{IE} > 1.0$) is dependent on its mixing pressure at Station 1 . P_P is less than ambient or secondary flow total pressure, P_{TS}. Accordingly, to produce thrust augmentation, diffusion must take place downstream of Station 1 to bring the low mixed flow static pressure up to the exit pressure P_E which is equal to ambient, P_{AMB}. There is an optimum mixing pressure P_1 which gives maximum augmentation and is controlled primarily by the mixed flow diffusion process and/or diffuser area ratio.

Payne's analysis was utilized to evaluate idealized ejector augmentation, ϕ_{IE}, using ERALS concept operating conditions and geometries. Although this analysis assumes incompressible flows, useful pumping characteristics and key velocity ratio trends are easily determined from a set of curves provided in Reference 1 and reproduced on Figures 22 through 24.

As shown in Figure 22, the analytical procedure is to evaluate ejector inlet-to-jet velocity ratio, V_I/V_J, by using ERALS primary and secondary flow characteristics and assuming values of entrainment ratio, N. The calculated velocity ratio is plotted as a function of entrainment ratio, Figure 24, and it intersects the analytically determined curve at an assumed value of diffuser efficiency, η_D, to determine the design point entrainment ratio, N. The evaluated entrainment ratio and diffuser efficiency are then used with Figure 23 to determine the idealized ejector augmentation ratio, ϕ.

In general, the actual design flowpath departs from the ideal shape necessary for realizing the best possible augmentation ratio. Therefore, derates must be established to account for nonideal ejector losses and to arrive at more realistic performance values. An accurate estimate of these losses can only be obtained by testing of detailed models.

Since test data were unavailable at this time, the performance derates were determined subjectively. The general approach was to visually note geometric variations from an ideal ejector flowpath and to them consider

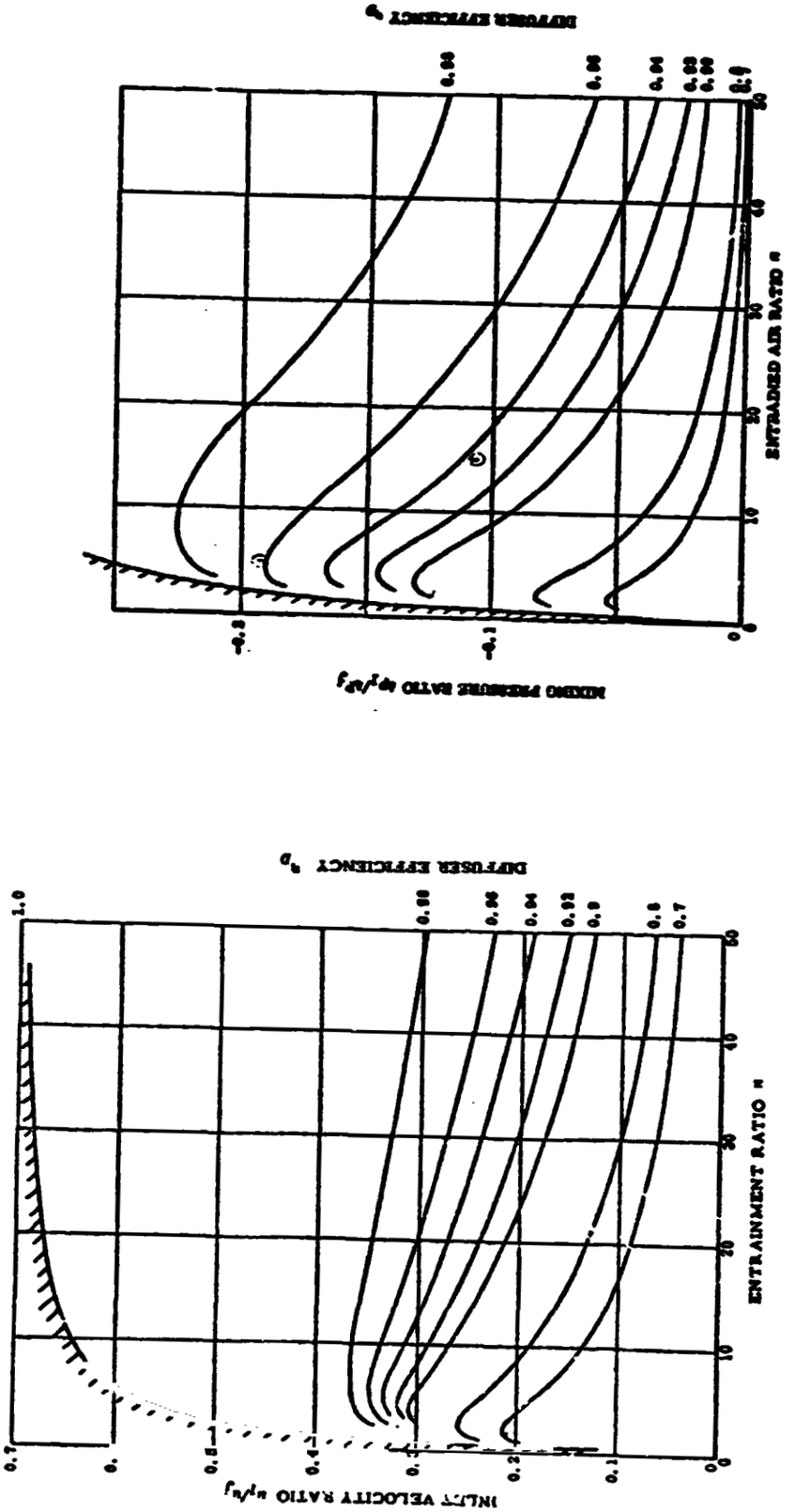

Figure 24. Idealized Ejector Performance Incompressible Flow Analysis.

feasible design improvements. The finalized relative augmentation ratios were calculated by using Design 1A augmentation ratio as a base value. Relative values of 1.00, therefore, represent an actual value that could be less than or more than unity depending on the flow losses of the design.

3.3.2 Selected Concept Analysis and Quantitative Losses

The selected concepts were evaluated using a more detailed analysis based on the methodology developed in Reference 7 and more completely outlined in Appendix A. As shown in Figure 25, this approach assumes one-dimensional compressible flow and obtains flow solutions for the primary and secondary flows in five regions. An assumed range of secondary flows is introduced in the inlet section to set the stage for obtaining a static pressure match at the end of the accommodation region which has been postulated to simplify the analysis.

The accommodation region considers only the merged behavior of the unmixed secondary and primary flows. The primary jet expands or contracts isentropically while the secondary flow accelerates to its entrainment Mach number. These processes take place between Sections 1 and 2 (Figure 25) until an accommodation between streams has been made by matched static pressure. The detailed methodology for this calculation is described in the Appendix.

A control volume is then set up in the constant area mixing region and mixed flow properties are determined based on enthalpy, momentum, and continuity relations. The mixed flow properties are used to calculate mixing section friction loss and this establishes the overall total pressure rise required by the secondary stream for the assumed conditions. Independent consideration of total pressure losses for the inlet, mixing, and diffuser sections establishes the total pressure rise that is necessary to satisfy loss assumptions.

For ERALS concepts, the mixing sections are short and calculated friction losses were negligibly small. The principal total pressure losses are therefore reduced to those associated with the inlet and diffuser sections. Inlet losses were simply assumed values of K_I (Table VI and Appendix section). Diffuser losses are dependent on the diffuser area ratio A_E/A_M and entrance conditions. The generalized diffuser loss correlation shown in Figure 26 was used to establish the diffuser loss factor K_D.

In general, these total pressure losses produce a mixed flow-to-ambient static-total pressure difference that increases parabolically as secondary flow increases as typified in Figure 27 for Model 2. The point at which this loss characteristic intersects with the pressure rise required by the flow determines the ERALS operating point. Augmentation ratio also increases as secondary flow increases as shown by the bottom graph in Figure 27. The operating point secondary flow established the ERALS augmentation as indiindicated.

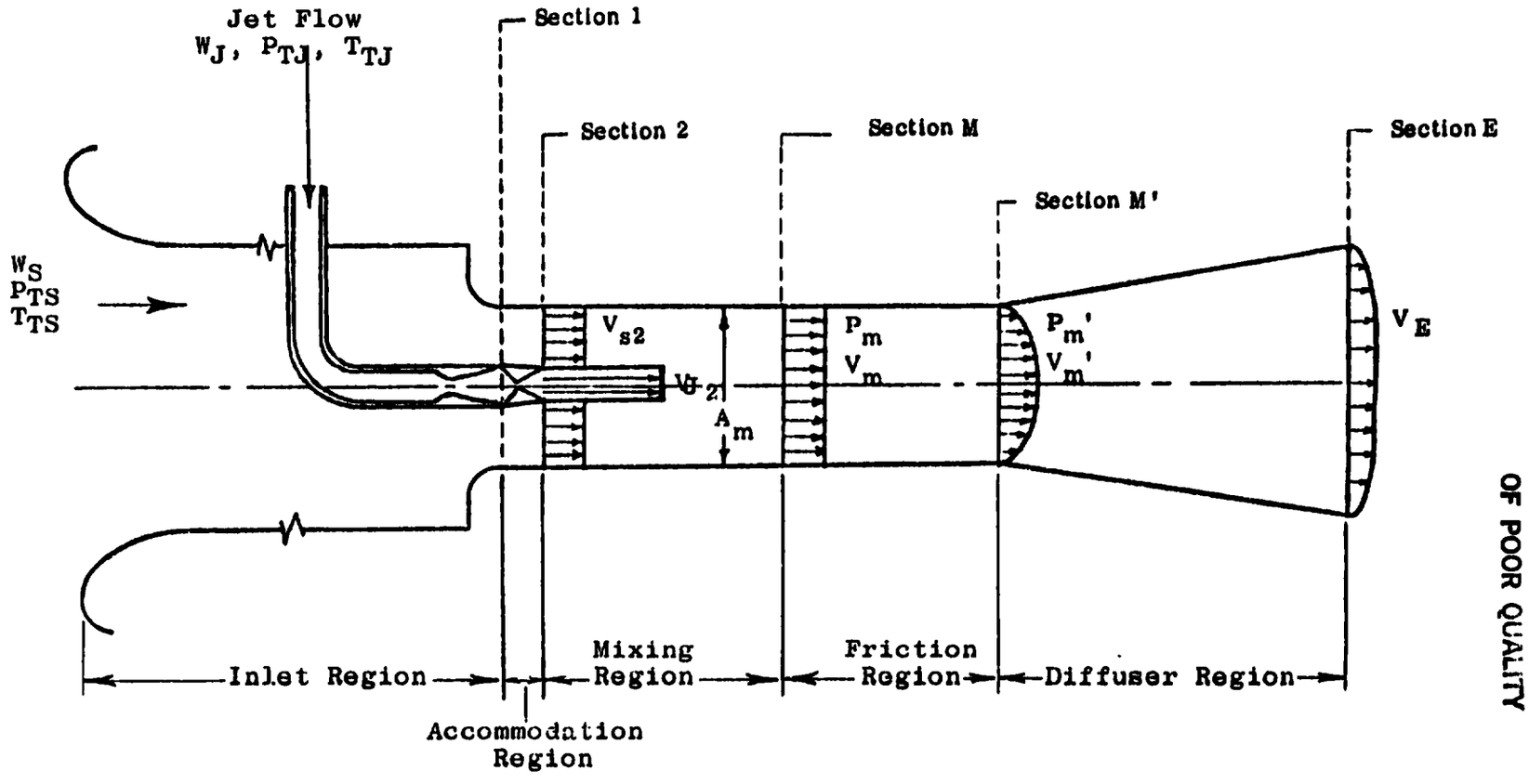

Figure 25. Analytical Model.

Table VI. ERALS Loss Factors and Performance Fully Mixed Flows.

$P_{TP}/P_{AMB} = 3.1$

$T_{TP} = 3260°$ R

Concept	A_M/A_P	A_E/A_M	Δ_D, degree	K_4	K_I	K_D	W_S/W_P	Δ_{PT}/P_{AMB}	ϕ
1	1.89	1.0	-	1.0	10.0	1.08	0.36	0.92	1.06
1	1.89	1.0	-	1.0	1.0	1.20	0.72	0.94	1.42
2	2.48	1.0	-	1.0	10.0	1.06	0.50	0.65	1.06
2	2.48	1.0	-	1.0	1.0	1.33	0.89	0.59	1.23
2	2.48	1.0	-	1.0	0.5	1.39	0.95	0.59	1.28
2	2.48	1.35	10	1.0	1.0	1.52	1.16	0.64	1.51
2	2.48	1.35	10	1.0	0.5	1.53	1.19	0.66	1.56
3	2.77	1.0	-	1.0	10.0	1.05	0.56	0.56	1.06
3	2.77	1.0	-	1.0	1.0	1.35	0.90	0.50	1.18
3	2.77	1.0	-	1.0	0.5	1.36	0.93	0.50	1.19
3	2.77	1.56	10	1.0	1.0	1.72	1.05	0.50	1.26
3	2.77	1.56	10	1.0	0.5	2.00	1.16	0.51	1.33

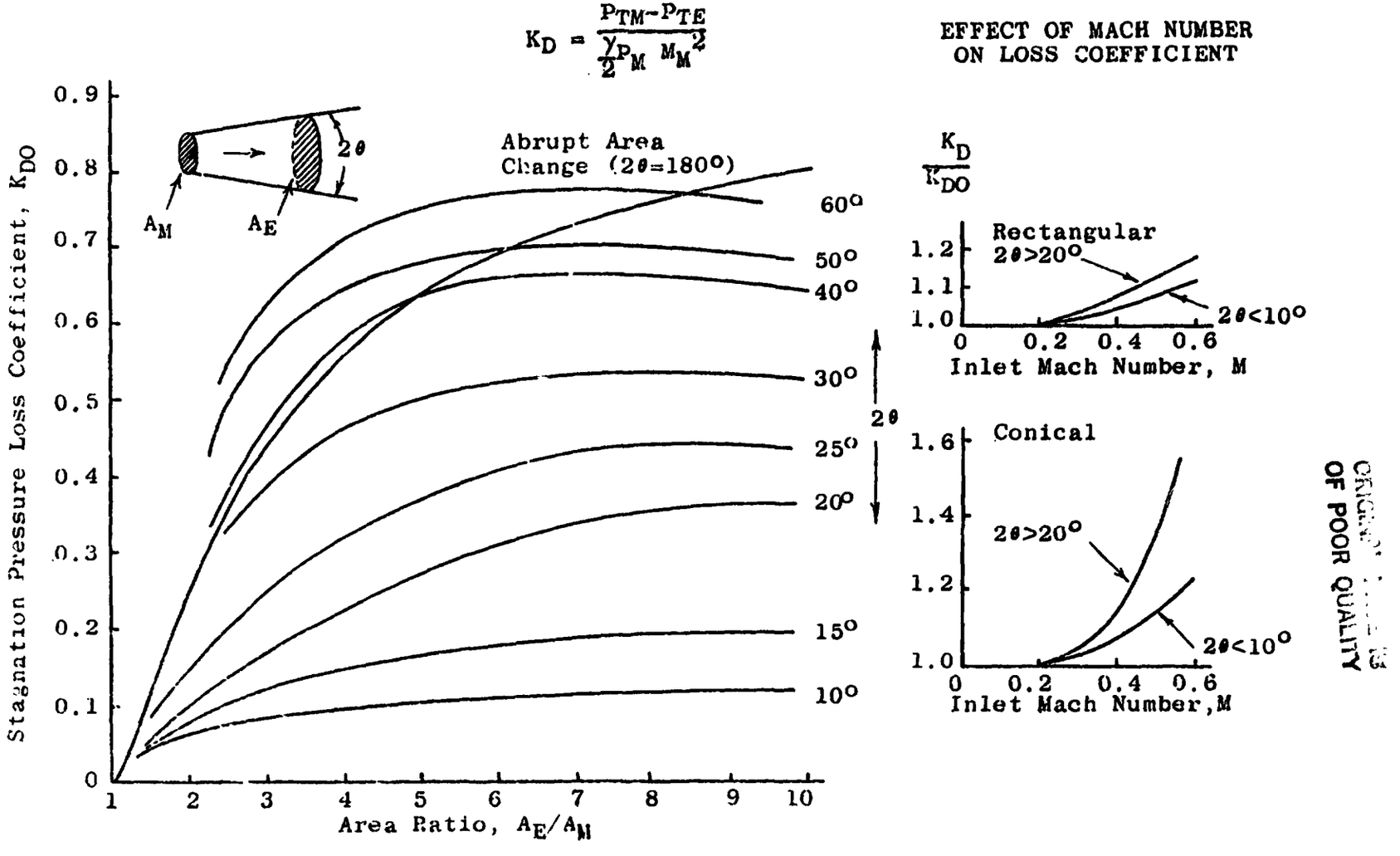

Figure 26. Loss Coefficients for Straight Conical Diffusers.

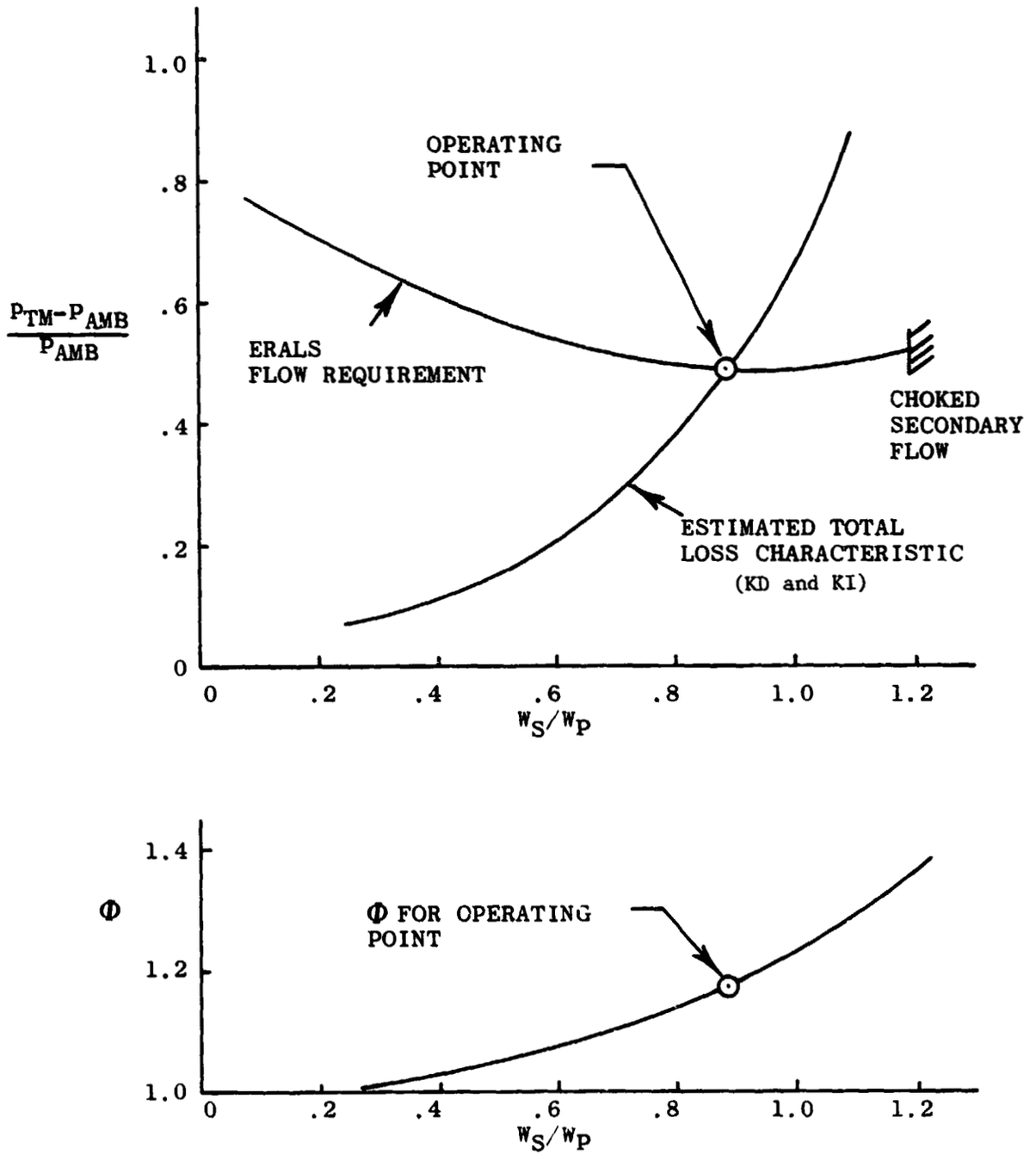

Figure 27. Method of Determining ERALS Operating Points, Model 2.

The greatest augmentation ratio occurs for concepts that entrain the most secondary flow. In general, the entrainment process is governed by the mixing capability and flowpath losses. The performance analysis described in Appendix A assumes a fully mixed flow and arbitrarily assigned pressure losses and does not constrain mixing in any way. However, the ERALS designs are all severely limited in this respect. Accordingly, to make the performance estimates more realistic, the analysis was extended to account for partial mixing.

The gross thrust of the ERALS system is a function of the flow total pressure and, therefore, of the pressure rise parameter $P_{TM} - P_{amb}/P_{amb}$. For the extended methodology, it was assumed that the partially mixed flow pressure rise is directly proportional to the fully mixed flow pressure rise. The constant of proportionality was furthermore assumed equal to the Frost mixing function, K_4, which is actually a thrust ratio and is derived in Reference 10. K_4 can be determined by the ERALS geometry and using the Frost correlation reprinted as Figure 28. On this basis, K_4 values of 0.15, 0.30, and 0.50 were determined for Concepts 1, 2 and 3, respectively.

The effect of reduced mixing is to shift the pressure rise function downward as shown in Figure 29. As a result, the ERALS operating point ① moves toward lower secondary-to-primary weight flow ratios and reduced augmentation ratio ② .

Figure 29 also demonstrates the effect of increasing inlet loss from $K_I = 1.0$ to $K_I = 10.0$. In this case, the loss curve moves toward the left ③ and also results in decreased weight flow ratio and augmentation ratio.

These analytic results are summarized in Table VI for various loss combinations. Concept 1 has no diffuser section as indicated by A_E/A_M. Concepts 2 and 3 were also evaluated without a diffuser. In addition, they were credited with a diffuser having a wall half angle of 10°. There were small differences in A_E/A_M due to geometric changes. Up to three K_I values, 10.0, 1.0 and 0.5, were assumed for inlet losses. Limitations in A_M/A_P prevented the evaluation of a matched pressure rise for Concept 1 with fully mixed flow. Consequently, its operating point was assumed to be at the choked secondary flow condition. Its augmentation ratio was estimated on this basis.

Diffuser geometry also significantly influences diffusion losses and, therefore, the operating point position. An efficient low loss diffuser permits the ERALS to produce lower pressure to initiate mixing and, therefore, entrain more secondary flow. Concepts 2 and 3 have adjustable diffuser flaps that can be set to provide more efficient diffusion. A flap divergence angle $\theta_D = 10°$ was assumed to be consistent with low diffuser loss.

The evaluated results are presented in Table VI for fully mixed flows and Table VII for partially mixed flows. In general, the highest augmentation ratio occurs for the greatest secondary flow, lowest inlet loss, and most efficient diffusion. The maximum values for fully mixed streams was achieved by

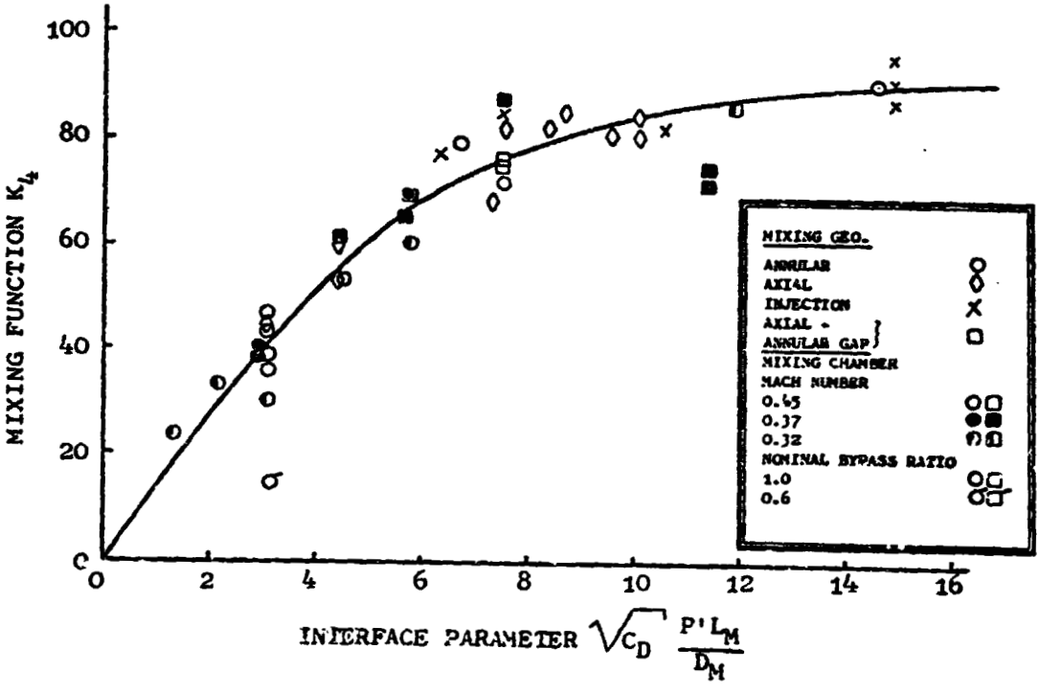

Figure 28. Mixing Function Correlation.

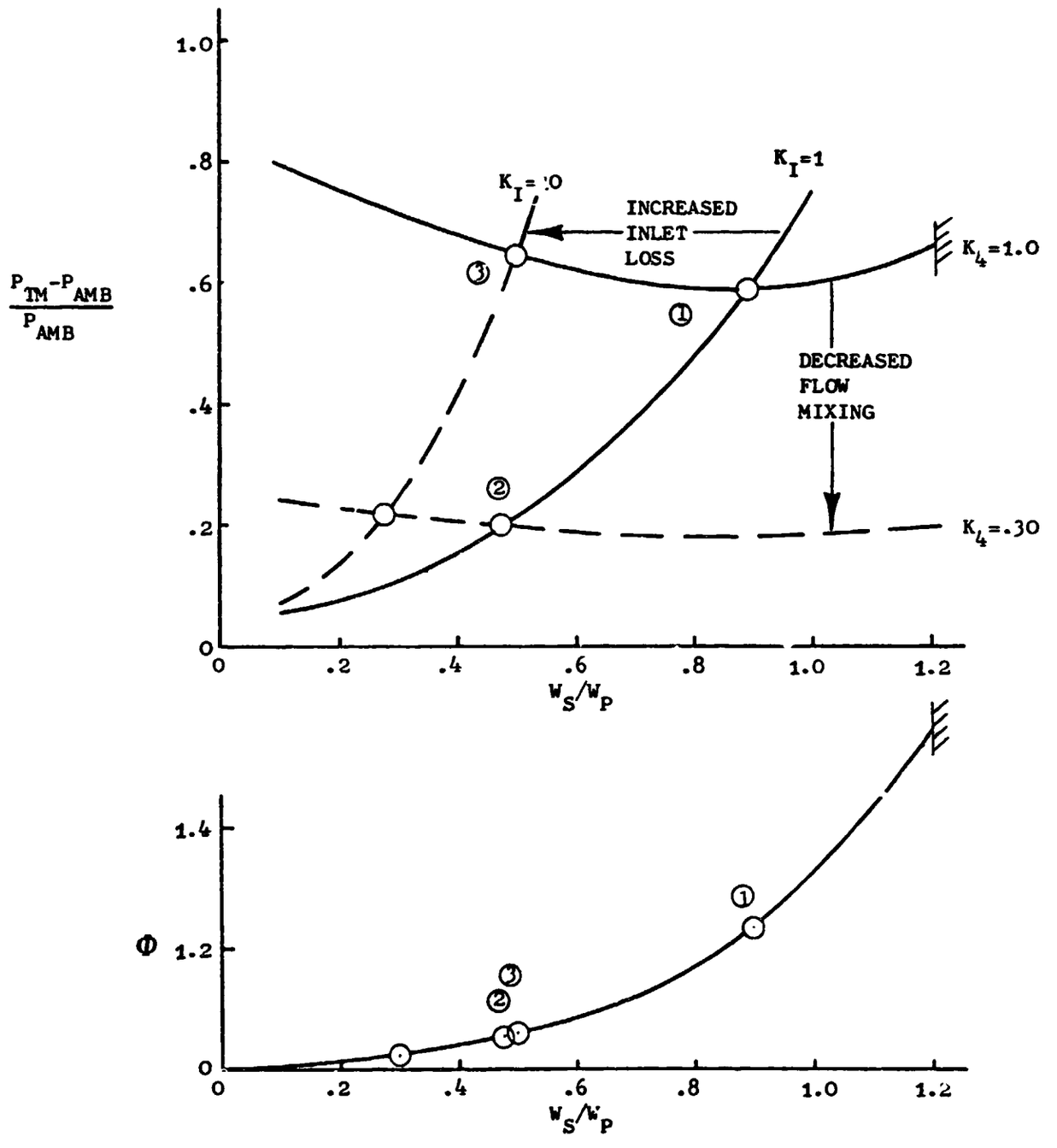

Figure 29. Effects of Inlet Loss and Flow Mixing on ERALS Operating Point, Model 2.

Table VII. ERALS Loss Factors and Performance.

$P_{TP}/P_{AMB} = 3.1$
$T_{TP} = 3260°$ R

Concept	A_M/A_P	A_E/A_M	θ_D, degree	K_I	K_D	W_S/W_P	$\Delta P_T/P_{AMB}$	ϕ
1	1.89	1.0	—	1.0	1.20	0.72	0.94	1.42
2	2.48	1.0	—	1.0	1.33	0.89	0.59	1.23
		1.0	—	0.5	1.39	0.95	0.59	1.28
		1.35	10	1.0	1.52	1.16	0.64	1.51
		1.35		0.5	1.53	1.19	0.66	1.56
3	2.77	1.0	—	1.0	1.35	0.90	0.50	1.18
		1.0	—	0.5	1.36	0.93	0.50	1.19
		1.56	10	1.0	1.72	1.05	0.50	1.26
		1.56		0.5	2.00	1.16	0.51	1.33

Concept 2 (ϕ = 1.56) followed closely by Concept 1 (ϕ = 1.42). When partial mixing is assumed, this trend is altered in favor of Concept 3 (ϕ = 1.18) which has most mixing (K_4 = 0.50). Although the partially mixed augmentation is considerably reduced when compared with the fully mixed flow values, the levels are still respectable and the entrained secondary flow substantial. It is clear that ERALS ejector performance is configuration dependent and sensitive to both the degree of mixing as well as amount of pressure loss in the system. In summary, the analysis shows that significant thrust augmentation is possible for the ERALS designs but further analytic and test evaluation is necessary to get more exact results.

3.4 PRELIMINARY DESIGN AND EVALUATION

Following concept evaluation, the decision was made to conduct preliminary design definition on the basis that the selected concepts can be installed in the NASA-Ames large-scale VEO model. This model, Figure 1, will have two nacelle-mounted vectorable nozzles and a simulated RALS system installed in the fuselage for pitch control.

Each of the three exhaust systems will be powered by GE J97 engines mounted in the nacelles and the fuselage. As a result, design parameters such as throat area and nozzle pressure ratio are somewhat different from those of General Dynamics R-104 aircraft design, which is the basis of the Ames VEO model. The J97 approach provides a forward/aft thrust split of approximately 33/67, whereas the R-104 requires a thrust split of 45/55. Since ERALS Concepts 1 and 2 were sized for twin jet installations and therefore represent one nozzle per engine in a two-engine system, they would require a "Y" duct from the single J97 engine to split the flow. On the other hand, Concept 3 was conceived as a single nozzle to be powered by merged flows from the two nacelle engines. Its simulation in the VEO model requires a direct duct connection to the single fuselage mounted J97. To simplify the complex ducting needed to accommodate all these possibilities, the decision was made to install all three ERALS concepts as single rather than twin and single exhaust systems.

The preliminary designs were evaluated using the more detailed ejector analysis described in the previous section and in the Appendix. The VEO installed ERALS also served as the basis for defining the geometry of small scale models for a testing at NASA-Lewis. The program elements are described in more detail in the following sections.

Preliminary design of the selected ERALS concepts began by redefining the VEO model fuselage sections. It was found that the original model lines required modification to install the fuselage-mounted GE-J97 and to duct air from the nacelle inlets. Early in this design process, the decision was made to generate layouts using the GE Interactive Graphics System rather than to use conventional drafting procedures. There were seveal reasons for this decision. Foremost, was the fact that scaling would eventually be necessary

to design approopriate scale models for the NASA-Lewis Test Program. In addition, changes in configuration were expected in both the Ames VEO model and in the ERALS installation. The Interactive Graphics System readily lends itself to changes in size and configuration. The preliminary design descriptions presented herein are portions of layouts developed using this approach. Duct sizes and envelope requirements were determined as part of the reference program.

Following fuselage definition, trial fits were made of the three ERALS concepts behind the cockpit section of the fuselage. This position corresponds with the aft-mounted RALS test system being designed under Contract NAS2-10556. A common duct was desired for the three selected ERALS concepts. Finalized installations were prepared in GE Drawing 4013269-379 and are shown in Figures 30, 31, and 32.

Concept 1, Figure 30, is axisymmetrical in shape with a pivotable jet flow nozzle. The same pivot is shared by a shroud which is shown in a side view together with the jet flwo nozzle in its VTOL mode. Area control is provided by a pari fo clamshell-type flaps (not indicated) on the nozzle. The nozzle and shroud may be pivoted independently to provide thrust vectoring from 15° forward to 30° aft. The nozzle is stowed by pivoting both nozzle and shroud within the fuselage envelope and closing the lower bomb bay doors and inlet doors. As an ejector, this system provides a relatively short mixing section for all vectored models. The five cross-sectional views indicate the complex distribution of secondary flow that is necessary to provide uniform conditions in the mixing section. The analysis of this type of ejector has shown that the inlet flow distribution will have a dominating influence on its performance. Similarly, the actual size of the mixing section will be much smaller than desired. This concept has only about half of a diffuser (formed by the bomb bay doors) and will suffer a dump loss, and therefore relatively low ejector performance.

Concept 2, Figure 31, has a two-dimensional pivotable nozzle for vectoring flow and a translating flap in the aft section of the nozzle for A_8 control. Except for change in shape, the inlet section is similar to that of Concept 1. A combined two-dimensional mixing and diffusing section is formed by independently controlled forward and aft flaps. This concept has a capability for vectoring thrust from 15° forward to 70° aft. Vectoring of the internal flow, however, can occur only at some expense to flow mixing and/or diffusion.

Concept 3, Figure 32, has a greater pumping capabilty than Concept 2 or 3 due to its smaller jet size and larger secondary flow area, A_M/A_P. This greater secondary flow area is obtained by passing the engine exhaust through an annular section approaching the nozzle throat and through a complex throat formed between the seven centrally positioned tubes. The secondary flow is pumped through the center of the system and through an outer annular area. In the VTOL mode, the secondary flow mixing and diffusion take place over a centrally located deflector vane and between the two bomb bay doors. The vane is positioned across three secondary flow ports to take advantage of cooling by secondary flow. Aft and forward vectoring is obtained by pivoting the

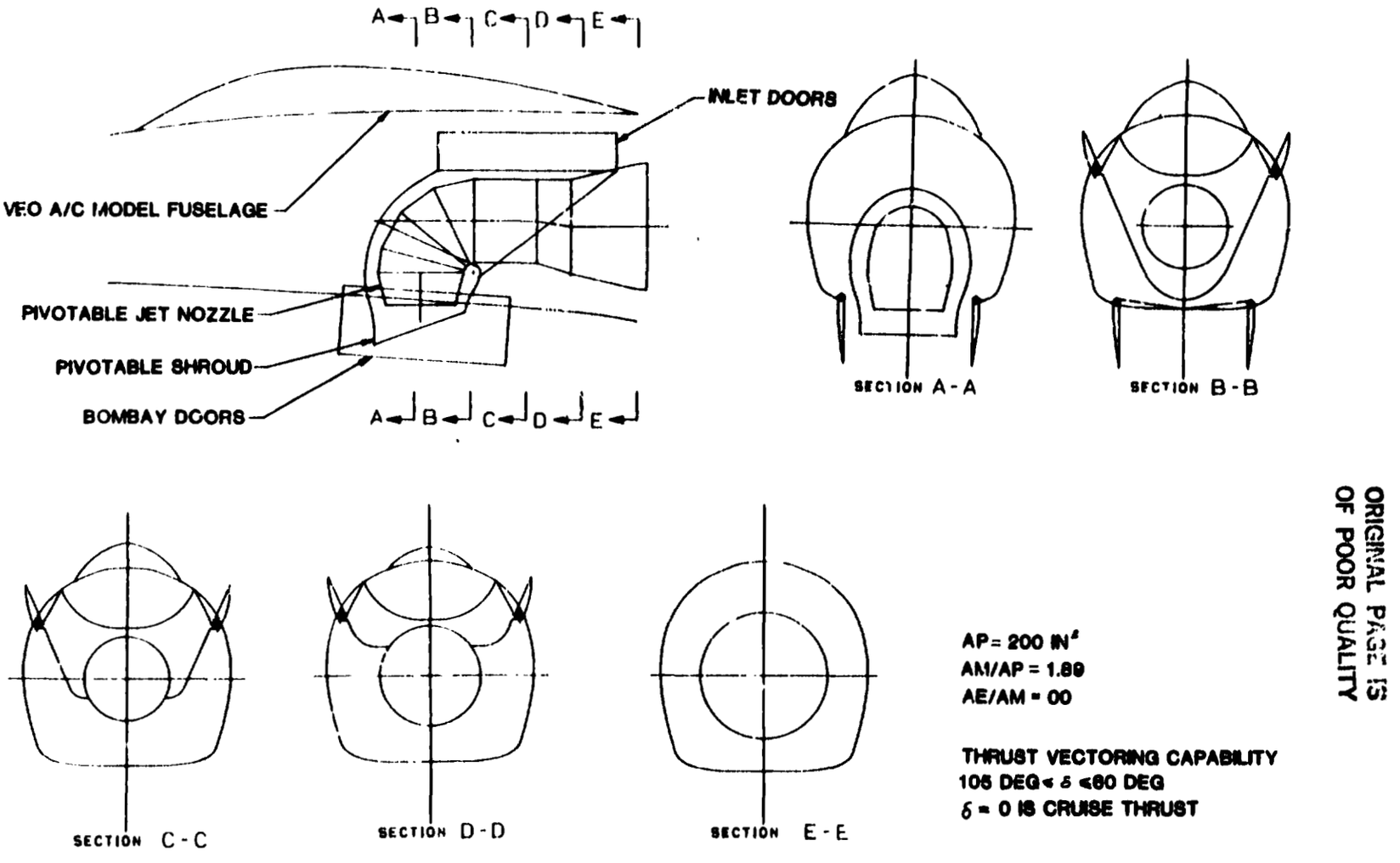

Figure 30. ERALS Selected Concept No. 1 Installed in NASA-Ames VEO A/C Model.

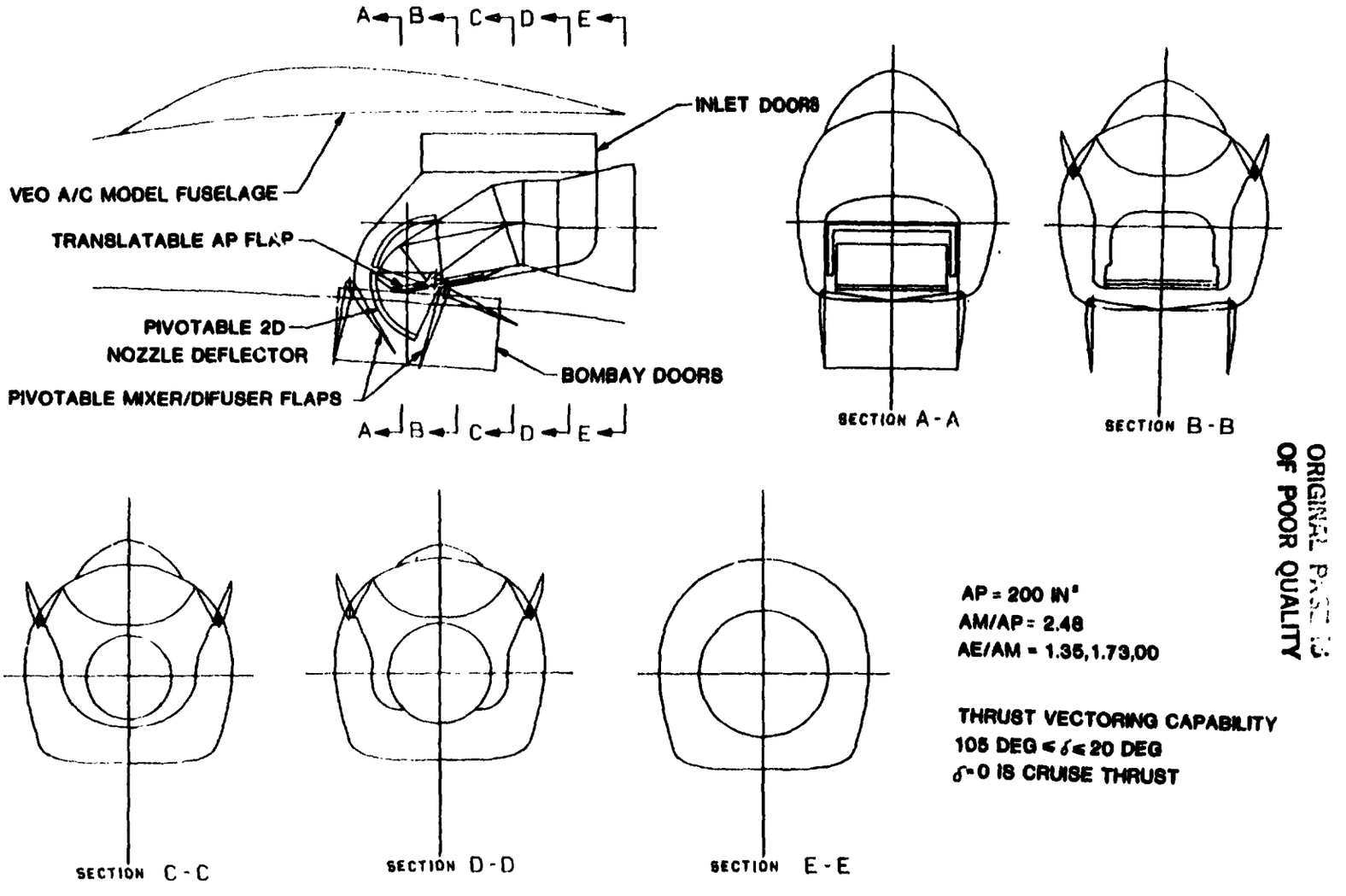

Figure 31. ERALS Selected Concept No. 2 Installed in NASA-Ames VEO A/C Model.

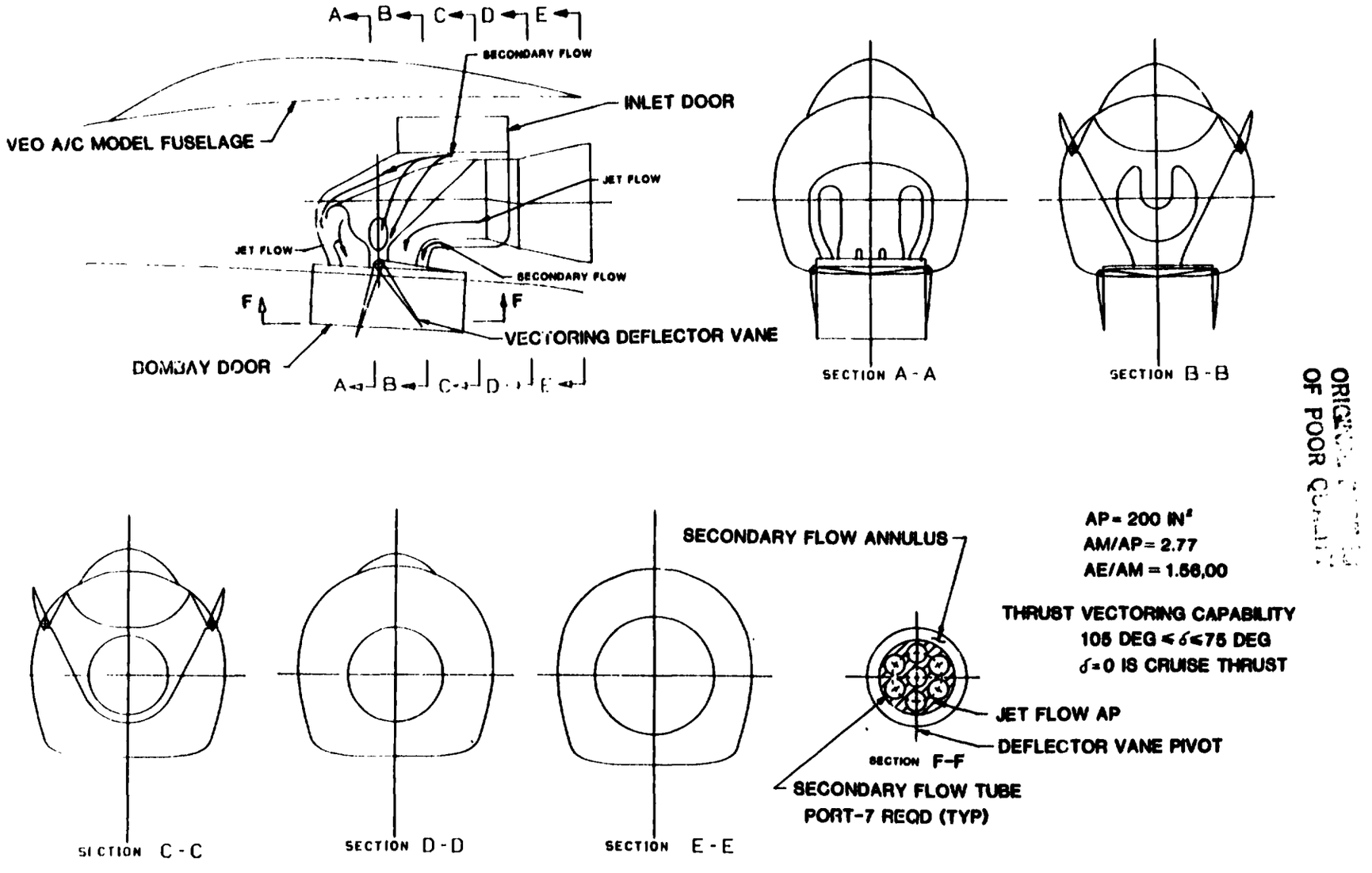

Figure 32. ERALS Selected Concept No. 3 Installed in NASA-Ames VEO A/C Model.

deflector. The amount of deflection capability is limited but should exceed ± 15°. These flaps would all be stowed, merging with fuselage lines when not in use.

As previously described, the installed ERALS designs have inlet, mixing, and diffuser sections which are considerably different than those usually postulated for analysis. Consequently, there are no data available for assessing ERALS losses and performance. Furthermore, due to the complex three dimensional asymmetric flows that are set up in these systems, a detailed analysis would be extremely difficult and could be carried out only by applying arbitrary assumptions. Therefore, model tests are necessary to generate any reliable ERALS performance data.

An appropriate test philosophy is demonstrated by the scale model layouts prepared in GE Drawing 4013269-390 and described in Figures 33, 34, and 35. The general test objectives would be to evaluate performance, determine component losses, and explore possible ERALS design improvements. Models in these layouts were sized for nominal hot gas characteristics supplied by a NASA-Lewis facility as follows:

Max. Flow = 60 lb/sec

Max. Hot Flow Total Pressure = 60 psia

Max. Hot Flow Total Temperature = 1660° R

Model Throat Area = 79 in.^{2}

Model Throat Diameter = 10 in.

On this basis, the ERALS test models would be scaled down to 63% of that required by the NASA-Ames VEO model and GE-J79 engine.

Concept 1 is simulated in the model layout shown in Figure 33. The inlet duct flowpath was exactly simulated for the baseline mode as represented in the side view by the solid lines. Additional inlet doors are provided for ventilating the secondary flowpath in areas which may be starved or separated. An important ejector parameter is the mixing section-to-jet flow area ratio, A_M/A_P. To establish performance sensitivity to this area ratio, a smaller jet tailpipe and jet area (dash lines) would replace that shown for the baseline. In addition, a two-piece mixing section extension (dash lines) may be attached to the shroud to determine the effect of constant area mixing length on performance. An axisymmetric conical diffuser is used with or without the mixing extension to determine its influence on ERALS operation.

Concept 2 model lines are shown in Figure 34. Except for the pivoting primary deflector, the model and full scale system are similar. The jet flow deflection is simulated by turned sections that are attached directly to the tailpipe. The baseline model for Concept 2 has pivoting forward and aft deflector flaps for simulating variable area ratios and controlling secondary

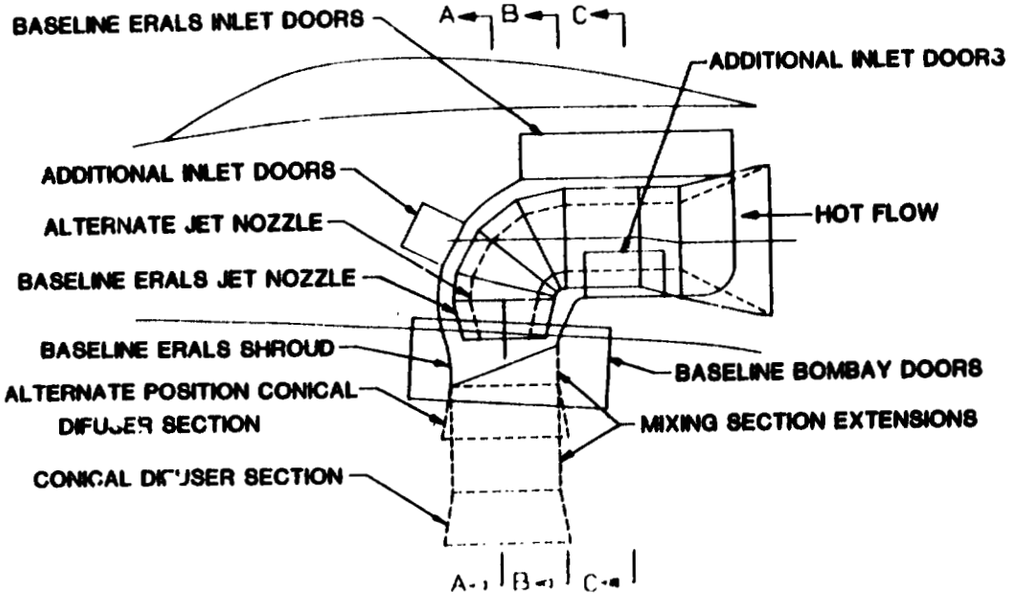

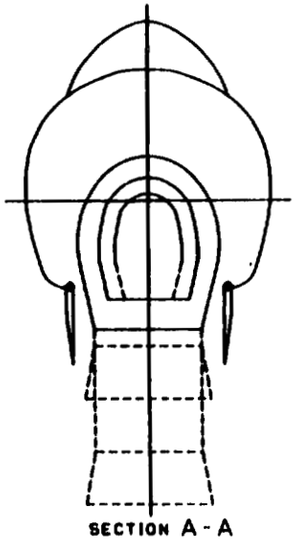

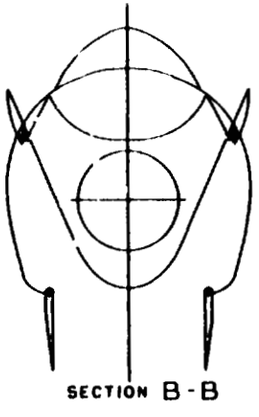

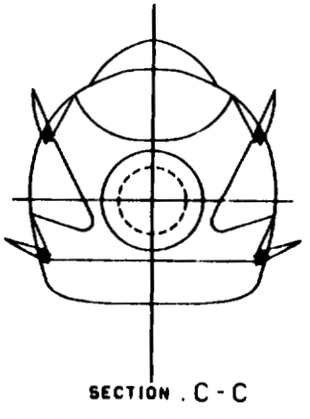

CONFIGURATION	AP IN²	AM/AP	AE/AP	δ
BASELINE	79	1.89	00	90
ALTERNATE	39.5	3.78	00	90

TTP MAX = 1660 DEG R

PTP MAX = 60 PSIA

Figure 33. ERALS Scale Model Concept No. 1.

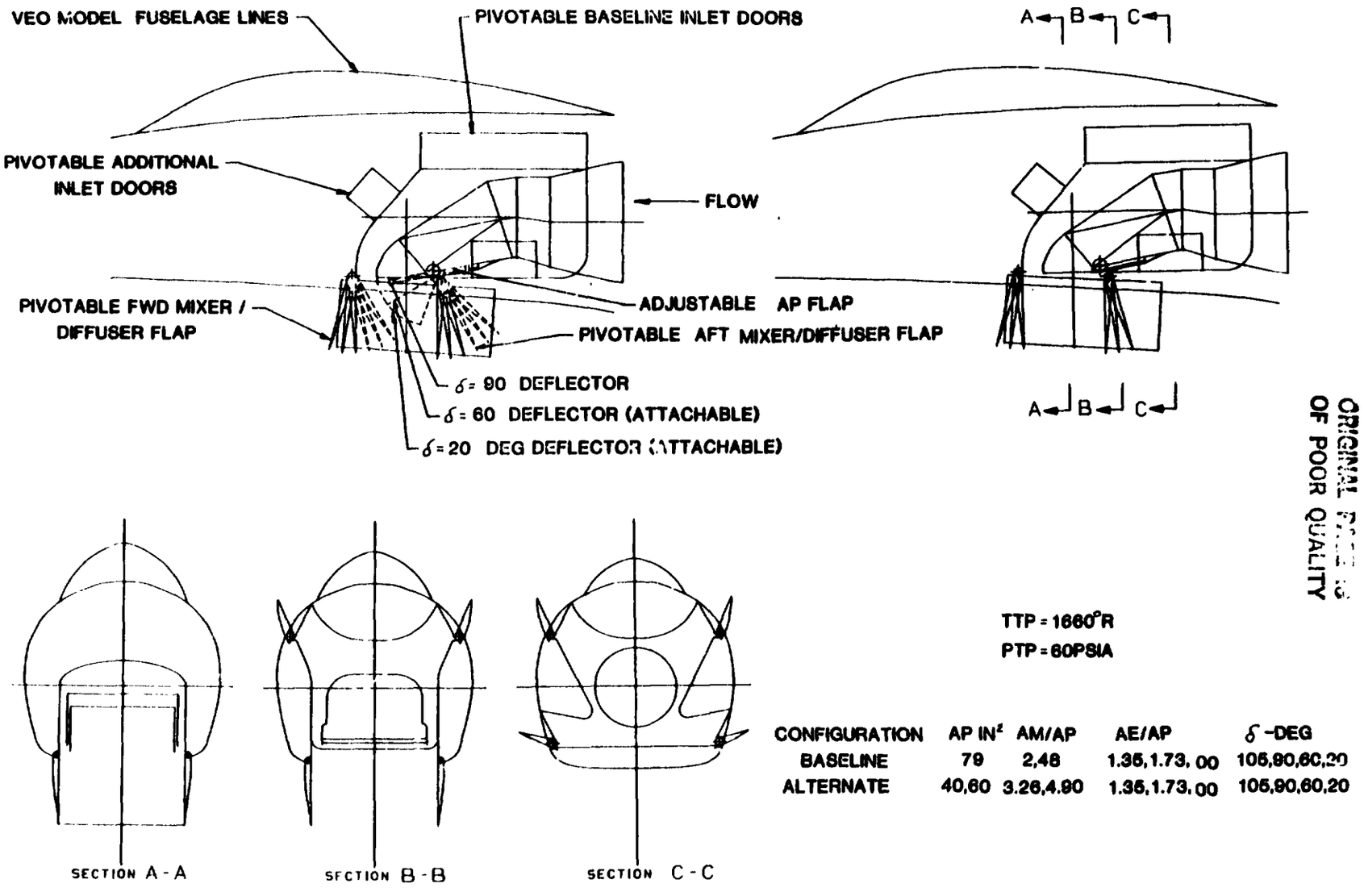

CONFIGURATION	AP IN²	AM/AP	AE/AP	δ -DEG
BASELINE	79	2,48	1.35,1.73, 00	105,90,60,20
ALTERNATE	40,60	3.26,4.90	1.35,1.73, 00	105,90,60,20

Figure 34. ERALS Scale Model Concept No. 2.

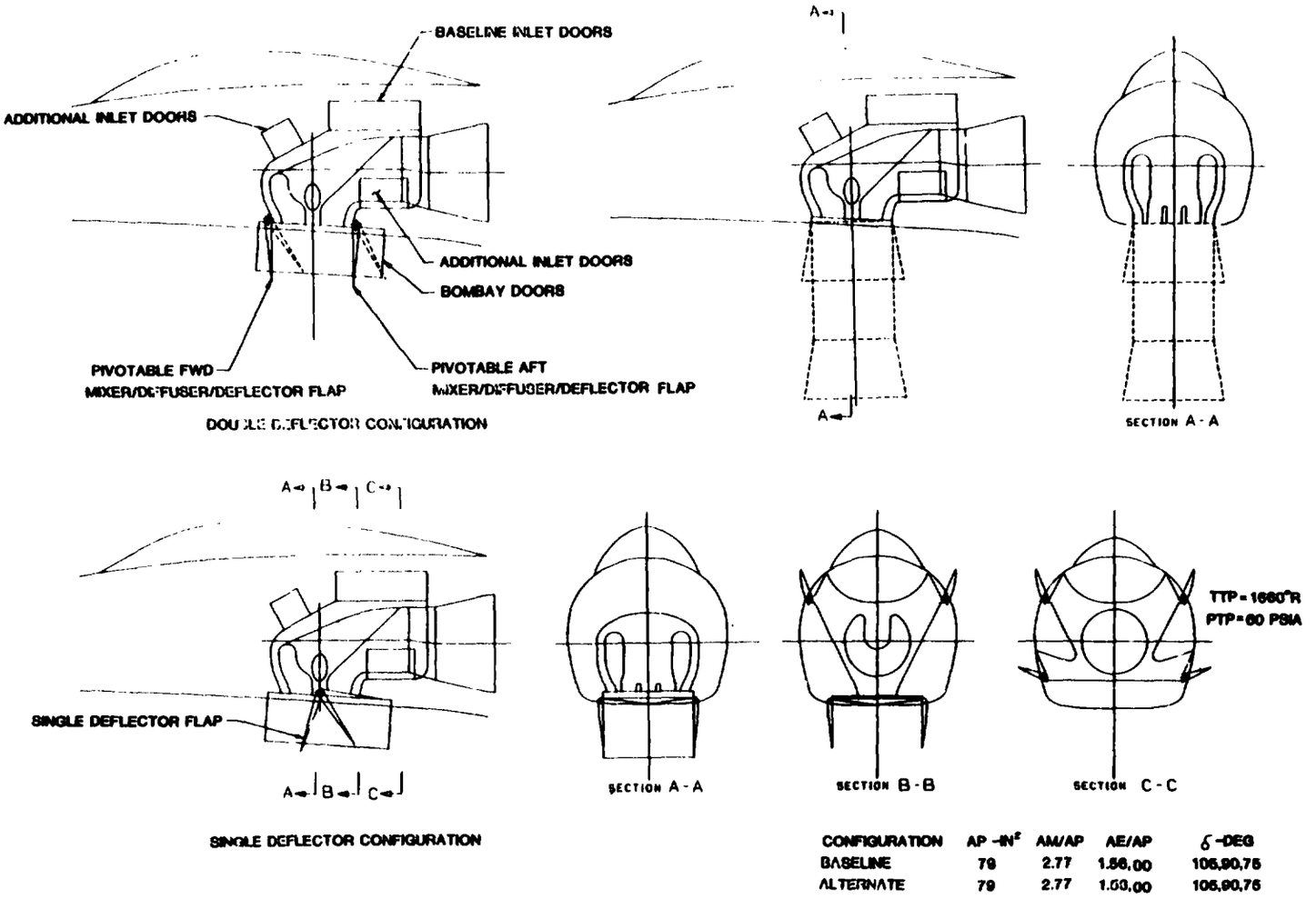

CONFIGURATION	AP - IN^2	AM/AP	AE/AP	δ - DEG
BASELINE	79	2.77	1.56,00	105,90,75
ALTERNATE	79	2.77	1.53,00	105,90,75

Figure 35. ERALS Scale Model Concept No. 3.

flow during deflection. As an alternate vectoring approach, the jet flow tailpipe could be tested without any pivotable flow deflector with the diffuser flaps used for vectoring the mixing and diffusing flow. Additional vents are shown for improving inlet flow performance.

Concept 3 model is shown in Figure 35. The final preliminary design for this concept uses a single vane for deflecting the flow. It is proposed that this model be tested with forward and aft flaps replacing the cental vane to establish how important this more complete mixer and diffuser section is compared to the simpler single vane. In addition, the flaps could be removed and a round conical diffuser attached to the nozzle. This would provide a comparison of performance for a round versus square diffuser system. The conical diffuser could then be replaced with a round cylindrical mixing section that can be tested with and without a conical diffuser thus simulating more nearly an idealized ejector. Additional doors are shown at the bottom of the inlet duct to relieve pressure loss in this local area.

The primary figure of merit used for ejector performance is in its augmentation ratio. This is defined as the total thrust generated by the system divided by the thrust of the jet flow alone expanded to ambient pressure. Since the augmentation ratio relies on force evaluations, it is desirable to have these tests conducted with the models on a force balance. Extensive pressure and temperature instrumentation should be supplied to provide detailed flow information and to cross check force balance results; in addition, all three concept models should be calibrated to thoroughly establish their secondary flow rates. These calibrations should be carried out at simulated operating conditions by pumping secondary flows through the model at below atmospheric static pressures.

System component losses should be established in terms of factors (K_I, K_{FR}, K_D) used in the analytic treatment and defined in the List of Symbols and Appendix. In this way, the analysis with its calibrated factors can be applied to predict the effects of changes in design and define optimum configurations as well as their performance possibilities.

4.0 RESULTS

This study has identified three potentially useful ejector concepts for use on a remote exhaust nozzle. The first concept adds as ejector shroud and the necessary inlet and discharge ducts and doors to a variable area, pivoting primry nozzle. This concept has the capability of providing side vectoring as well as limited fore and aft vectoring, providing a means to control yaw in vertical takeoff or hovering flight condition.

The second concept adds the ejector features to a hooded RALAD-type vectoring nozzle, providing much greater aft-vectoring capability at the expense of side-vectoring capability. Such a nozzle design is of greater interest for a STOL aircraft that uses the aft-vectoring capability to enhance its initial takeoff acceleration.

The third concept utilizes multiple secondary air injection tubes to achieve a much longer interface between the primary and secondary streams. Although this nozzle is relatively bulky and does not lend itself to thrust vectoring, it is expected to provide a much greater thrust augmentation ratio than the first two concepts.

A search of existing literature provides a basis for analysis of the new ejector concepts. However, each of the concepts involves a complex three-dimensional flow field and severe geometric constraints on the inlet, mixing section, and diffuser. No data could be found that would permit an accurate assessment of the pressure losses in these critical components. Consequently, model testing is necessary to determine the augmentation capability of the concepts with any degree of accuracy.

By utilizing the fuselage contours of the NASA-Ames Large Scale VEO Fighter Model, realistic geometric constraints have been applied to each of the ejector concepts. By scaling the resulting installations down to a size that means NASA-LeRC facility capability, a very worthwhile test program could be conducted at reasonable cost. Several alternate pieces of hardware have been identified for model testing to evaluate the effect of important parameters such as diffuser length and mixing length. Model testing would, in addition to defining the thrust augmentation capability of the selected ejector concepts, provide much needed data on their jet mixing and footprint temperature characteristics.

5.0 CONCLUSIONS AND RECOMMENDATIONS

Because of the continuing interest in V/STOL, particularly in STOL fighters, the RALS propulsion concept remains a viable contender. Several concerns arise from an inadequate data base. These include the exhaust footprint temperature level and distribution, and the problems associated with cooling the aircraft bay adjacent to the pilot and electronics suite. Propulsion system thrust-to-weight ratio is a major driver in any STOL or VTOL system, and any means of enhancing lift/thrust is of potential value. The three ejector concepts selected in this study all address the above problems to varying degrees.

Although past ejector test and development experience has not all been favorable, exhaust ejectors have been used very successfully on the J79 and other engines. For use on a remote exhaust nozzle, high augmentation ratios may not be achievable by ejectors meeting the stringent geometric limitations imposed by the fuselage stowage requirement. But, even modest augmentation ratios could be very desirable when accompanied by improvements in aircraft cooling and jet mixing.

A problem that has been concountered in previous developments is in scaling the design from model size to actual size. Real tolerances, surface finishes, and fits can adversely affect diffuser performance. Large stability margins are required to avoid separation and to ensure predictable performance of the final designs.

Based on the results of this study, a scale model test program is recommended. This program could be conducted by NASA or under contract to NASA. The primary objectives would be to explore the performance characteristics of the selected ejector concepts and to assess their cooling and jet mixing capability. If one or more of the concepts should prove to be attractive on the basis of the small scale model test, a larger model could be build and tested in the NASA-Ames Large-Scale VEO Fighter Model. This approach would permit scale effects to be evaluated directly, ensuring the acquisition of a valid data base for future aircraft use.

6.0. LIST OF SYMBOLS, ACRONYMS AND CONVERSIONS

A	Area, $in.^2$
A^*	Choked Flow Area, $in.^2$
C_D	Nozzle Flow Coefficient
C_F	Friction Coefficient
C_P	Specific Heat at Constant Pressure, Btu/lb - ° F
D	Diameter, in.
FARM	Fuel/Air Ratio for Mixed Flow
FARP	Fuel/Air Ratio for Primary Flow
g	Gravity = 32.174 ft/sec
h	Enthalpy, Btu/lb
H	Jet Height, in.
J	Energy Conversion Factor = 778,2 ft-lb/Btu
K_D	Diffuser Loss Factor
K_{FR}	Mixing Section Friction Loss - $2\ C_F\ L_M \sqrt{\frac{\pi}{A_M}}$
K_I	Inlet Duct Loss Factor - $P_{T5} - P_{T51}/qsi$
K_4	Frost Mixing Function
L	Length, in.
M	Mach Number
N	Entrainment Ratio
P	Static Pressure, psia
P'	Jet Parameter, inch
P_S	Specific Excess Energy for Combat Maneuverability
P_T	Total Pressure, psia
q	Dynamic Pressure, psia
R	Gas Constant - 1716.3 $\frac{ft^2}{sec^{2-\circ} R}$

T	Static Temperature, ° R
T_T	Total Temperature, ° R
V	Velocity, ft/sec
W	Gas Flow, lb/sec
γ	Specific Heat Ratio = 1.4
Δ	Total Pressure Difference, psia
δ	Vector Angle from Vertical, degrees
η	Efficiency
θ	Diffuser Wall Angle, degrees
ρ	Density, lb/ft^3
ϕ	Augmentation Ratio = Mixed Flow Gross Thrust/Primary Flow Gross Thrust

Subscripts

A	Air
AMB	Ambient
D	Diffuser
E	Exit
F	Fuel
I	Inlet
IE	Idealized Ejector
M	Mixed
P	Primary Jet
Ref	Reference
S	Secondary

ACRONYMS

ADEN	Augmented Deflector Exhaust Nozzle
ERALS	Ejector RALS
RALAD	RALS/ADEN
RALS	Remote Augmented Lift System
TOGW	Takeoff Gross Weight
VEO	Vectored Engine Over-Wing
V/STOL	Vertical/Short Takeoff and Landing
VTO	Vertical Takeoff

CONVERSIONS

English to Standard International Units

mass	lb x 0.4536 = kg
force	lb x 4.448 = N
distance	ft x 0.3048 = m
distance	nmi x 1.852 = km
distance	in. x 2.54 = cm
area	ft^2 x 0.0929 = m^2
area	$in.^2$ x 6.4516 = cm^2
area	acres x 0.04047 = km^2
Volume	$in.^3$ x 16.387 = cm^3
Volume	ft^3 x 0.0283 = m^3
Volume	gal x 0.003785 = m^3
velocity	ft/sec x 0.3048 = m/sec
velocity	knots x 0.51444 = m/sec
Power	hp x 745.7 = W
Temperature	(° F + 460) x 5/9 = ° K
Heat	Btu x 1055.9 = J
Airflow	lb/sec x 0.4536 = kg/sec
thrust	lb x 4.448 = N
sfc	lb/hr/lb x 0.0283 = g/sN
F_N/W_t	lb/lb x 9.806 = N/kg
F_N/W_a	lb/sec lb x 9.806 = Ns/kg
wt/area	lb/ft^2 x 4.877 = kg/m^2
Heat Load	Btu/lb x 2327.8 = J/kg

Pressure or Stress	psia x 0.6895 = N/cm^2
torque	in.-lb x 11.3 = cm N
torque	ft-lb x 1.356 = m N
Vol Flow	gpm x 63.0 = cm^3/sec
Heat Flow	Btu/min x 17.6 = J/sec
Unit Load	lb/in. x 1.75 = N/cm
Density	lb/ft^3 x 16.028 = kg/m^3

APPENDIX - COMPRESSIBLE FLOW ANALYSIS OF EJECTORS

The calculations outlined below were performed on an assumed analytic model shown schematically in Figure 25. The computations provide a complete description of flow properties at the beginning and end stations of five flow regions. Mixed flow characteristics were then used to determine ERALS design performance in the form of augmentation ratio.

The following assumptions have been assumed to simplify calculations:

1. Specific heat ratio, γ, was constant and equal to 1.4 for both jet and secondary flows. It should be noted that γ influences compressible flow relations significantly. Furthermore, the assumed jet temperature of 3260° F is at a lever where γ can be considerably less than 1.4 and can have significance on augmentation ratio. However, the importance of considering γ changes was waived on the basis that all models would be equally affected and therefore relative performance comparisons would still be valid.

2. No heat is transferred across walls of the ERALS designs.

3. Mixing takes place in an unlimited length constant area section and flows are completely mixed entering the diffuser. ERALS design mixing sections are shorter than required for complete mixing. The amount of mixing and its effects can only be determined experimentally.

Accommodation Region Solution

M_{S2} is determined from compressible flow and continuity relations

$$\frac{\frac{W_S}{W_P}\ W_P\ \sqrt{T_{TS}}}{P_{S1}\ (A_M - A_{S1})} = g\sqrt{\frac{\gamma}{R}}\ M_{S2}\ \left(1 + \frac{\gamma - 1}{2}\ M_{S2}\right)^{1/2} \tag{1}$$

where all terms except M_{S2} are known constants or assumed values.

$$\text{then} \quad P_{S2} = P_{TS}\ \left(1 + \frac{\gamma-1}{2}\ M_{S2}^2\right)^{-\frac{\gamma}{\gamma-1}} = P_{P2} \tag{2}$$

$$\text{and} \quad M_{P2} = \left[\frac{2}{\gamma-1}\ \left(\left(\frac{P_{P2}}{P_{TP2}}\right)^{-\frac{\gamma-1}{\gamma}} - 1\right)\right]^{1/2} \tag{3}$$

M_{P2} is then used to evaluate jet flow area A_{P2}

$$A_{P2} = \frac{W_P \sqrt{T_{TP}}}{P_{P2}\, g \sqrt{\frac{\gamma}{R}}\, M_{P2} \left(1 + \frac{\gamma-1}{2} M_{P2}^2\right)^{1/2}} \tag{4}$$

and

$$A_{S2} = \frac{\frac{W_S}{W_P} W_P \sqrt{T_{TS}}}{P_{S2}\, g \sqrt{\frac{\gamma}{R}}\, M_{S2} \left(1 + \frac{\gamma-1}{2} M_{S2}\right)^{1/2}} \tag{5}$$

A test is made to determine if the calculated areas are in agreement with the ERALS geometric A_M

$$A_M \stackrel{?}{=} A_{P2} + A_{S2} \tag{6}$$

If not, a new M_{S2} is tried in equation (2). The calculations and test are repeated until equation (6) holds. The last values of M_{S2}, M_{P2}, P_{S2}, P_{P2} are the matched static pressure characteristics at Station 2.

Mixing Region Calculations

To determine the mixed flow solution a control volume was set up between Section 2 and Section M.

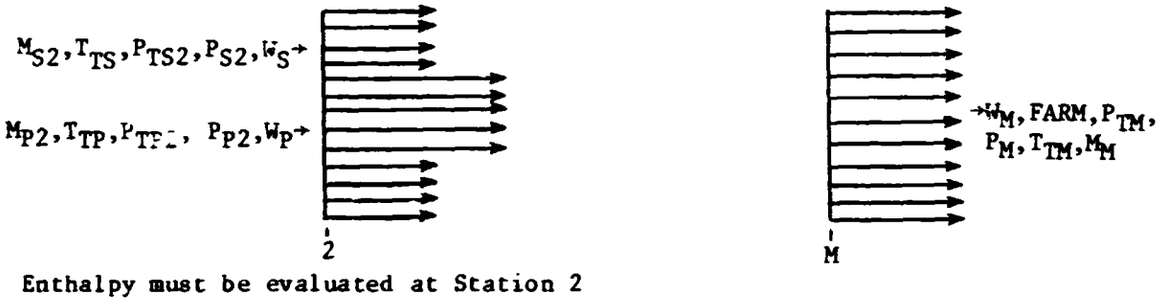

Enthalpy must be evaluated at Station 2

$$T_{P2} = T_{TP} \left(1 + \frac{\gamma-1}{2} M_{P2}^2\right)^{-1} \tag{7}$$

$$C_{PP2} = \frac{C_{PA} + FARP\, C_{PF}}{+ FARP} \tag{8}$$

where C_{PA} and C_{PF} are specific heats of air and fuel, respectively, and their value is dependent on static temperature

then

$$H_{P2} = C_{PP2} T_{P2} - \frac{M_{P2} \gamma RT_{P2}}{2gJ} \tag{9}$$

Similarly for the secondary flow

$$T_{S2} = T_{TS} \left(1 + \frac{\gamma - 1}{2} M_{S2}^2\right)^{-1} \tag{10}$$

$$H_{S2} = C_{PS2} T_{S2} + \frac{M_{S2}^2 \gamma RT_{S2}}{2gJ} \tag{11}$$

where

$$C_{PS2} = C_{PA} \tag{12}$$

for the mixed flow

$$FARM = \frac{FARP}{1 + (1 + FARP)\frac{W_S}{W_P}} \tag{13}$$

the mixed flow enthalpy is determined from energy considerations

$$H_M = \frac{W_S H_{S2} + W_P H_{P2}}{W_M} = C_{PM} T_M + \frac{M_M^2 \gamma RT_M}{2gJ} \tag{14}$$

where

$$C_{PM} = \frac{C_{PA} + FARM\ C_{PF}}{1 + FARM} \tag{15}$$

and M_M is calculated from a momentum balance between Stations 2 and M as outlined below.

Since C_{pM} and C_{pF} are a function of T_M, an iterative process must be used to determine the T_M and C_{pM} that agree with H_M.

The mixed flow static pressure, P_M, is based on the equation of state

$$P_M = \int_M RT_M = \frac{W_M}{g A_M M_M} \sqrt{\frac{RT_M}{\gamma}} \tag{16}$$

then M_M is determined from a momentum balance between Stations 2 and M.

$$\frac{W_M}{g} M_M \sqrt{\gamma RT_M} + P_M A_M = \frac{W_P}{g} M_{P2} \sqrt{\gamma RT_{P2}} + P_{P2} A_{P2} + \frac{W_S}{g} M_{S2} \sqrt{\gamma RT_{S2}} + P_{S2} A_{S2} \tag{17}$$

Reordering terms and substituting for P_M a quadratic equation in M_M is formed

$$\frac{W_M}{g} \sqrt{\gamma RT_M} M_M^2 - \left(\frac{W_P}{g} M_{P2} \sqrt{\gamma RT_{P2}} + P_{P2} A_M + \frac{W_S}{g} M_{S2} \sqrt{\gamma RT_{S2}}\right) M_M + \frac{W_M}{g} \sqrt{\frac{RT_M}{\gamma}} = 0 \tag{18}$$

After evaluating M_M, the rest of the mixed flow properties are calculated

$$T_{TM} = T_M \left(1 + \frac{\gamma-1}{2} M_M^2\right) \tag{19}$$

$$P_M = \frac{W_M}{g A_M} \sqrt{\frac{RT_M}{\gamma}} \tag{20}$$

$$P_{TM} = P_M \left(1 + \frac{\gamma-1}{2} M_M^2\right)^{\frac{\gamma}{\gamma-1}} \tag{21}$$

The total pressure rise required to pass the assumed amount of secondary flow without any system losses becomes:

$$\frac{\Delta PT}{P_{AMB}} = \frac{P_{TM}-P_{AMB}}{P_{AMB}} \tag{22}$$

Definition of Augmentation Ratio

For purposes of this program augmentation ratio, Φ is the total momentum of the primary and secondary flows normalized by the ideal momentum of the primary flow

$$\Phi = \frac{W_S V_{S2} - W_P V_{P2}}{W_P V_P} \tag{23}$$

where the ideal primary flow velocity, V_P, is

$$V_P = M_P \sqrt{\frac{\gamma R T_{TP}}{(1+\frac{\gamma-1}{2} M_P^2)}} \tag{24}$$

$$M_P = \sqrt{\frac{2}{\gamma-1} \left[\left(\frac{P_{TP}}{P_{AMB}} \right)^{\frac{\gamma-1}{\gamma}} - 1 \right]} \tag{25}$$

Determination of Total Pressure Loss

Inlet duct loss is defined in terms of Station 1 conditions:

$$\frac{\Delta P_{TF}}{P_{AMB}} = \frac{\gamma}{2} K_I M_{S1} \frac{P_{S1}}{P_{AMB}} \tag{26}$$

where

$$K_I = \frac{\Delta p_{TI}}{qS1} = \frac{P_{TS}-P_{TS1}}{qS1} \tag{27}$$

and M_{S1} is determined from

$$g\sqrt{\frac{\gamma}{P}}\ M_{S1}\ \left(1+\frac{\gamma-1}{2}M_{S1}^{2}\right)^{-\frac{\gamma+1}{2(\gamma-1)}} = \frac{\frac{W_S}{W_P}\ W_P\ \sqrt{T_{TS}}}{P_{TS}\ (A_M-A_P)} \tag{28}$$

then

$$P_{TS1} = P_{TS} - \frac{\gamma}{2}\ M_{S1}^{2}\ P_{S1} \tag{29}$$

where

$$P_{S1} = P_{TS}\ \left(1+\frac{\gamma-1}{2}\ M_{S1}^{2}\right)^{-\frac{\gamma}{\gamma-1}} \tag{30}$$

Mixing region t. ion loss is defined by mixed flow properties and assuming the mixed flow passes through a section with a length, L_M, equal to the actual mixing section. On this basis, the pressure loss is

$$\frac{\Delta P_{TFR}}{P_{AMB}} = \frac{\gamma}{2}\ K_{FR}\ M_M^{W} = \frac{P_M}{P_{AMB}} \tag{31}$$

where

$$K_{FR} = C_F\ \frac{A_{WET}}{A_{REF}} = 2\ C_F\ L_M\ \sqrt{\frac{\pi}{A_M}} \tag{32}$$

For ERALS, the mixing sections are very short and calculated friction losses were small.

The diffuser loss is combined with the dynamic head at its exit to define

$$\frac{\Delta P_{TD}}{P_{AMB}} = \frac{\gamma}{2}\ K_D\ M_M^{2}\ \frac{P_M}{P_{AMB}} + \frac{P_E}{P_{AMB}}\left[\left(1+\frac{\gamma-1}{2}\ M_E^{2}\right)^{\frac{\gamma}{\gamma-1}}-1\right] \tag{33}$$

where for estimating purposes, it was assumed the $P_E = P_{AMB}$ and $M_E = M_M$.

Then the overall total pressure loss for the system is calculated by combining (26), (30), and (32).

$$\frac{\Delta P_T}{P_{AMB}} = \frac{\Delta P_{TI}}{P_{AMB}} + \frac{\Delta P_{TFR}}{P_{AMB}} + \frac{\Delta P_{TD}}{P_{AMB}} \qquad (34)$$

This is a function of secondary-to-primary flow ratio and is used with equation (22) to determine the operating point, Figure 27. The corresponding augmentation ratio is the estimated performance.

REFERENCES

1. "Variable Cycle Engine Evaluation for Supersonic V/STOL Fighter Final Summary Report," General Electric Company R73AEG599.

2. "Variable Cycle Engine Evaluations for Supersonic V/STOL Fighters," McDonnell-Douglas Corporation N00140-75-C-0034.

3. "Study of Aerodynamic Technology for V/STOL Fighter/Attack Aircraft - Phase I Final Report," Grumman Aerospace Corporation NASA CR-152129.

4. "Remote Augmentor Lift System/Variable Cycle Engine Trade Study Final Report," General Electric Company R80AEG455.

5. Payne, P.R., "Steady State Thrust Augmentors and Jet Pumps," VSAA VLABS Report TR66-18, 1966.

6. Hickman, K.E., Gilbert, C.B., and Carey, J.H., "Analytical and Experimental Investigation of High Entrainment Jet Pumps," NASA CR-1602, 1970.

7. Quinn, B., "Recent Developments in Large Area Ratio Thrust Augmentors, AIAA Paper 72-1174, 1972.

8. Viets, H., "Thrust Augmenting Ejectors," APL 75-0224, 1975.

9. "Design of a V/STOL Propulsion System for a Large-Scale Fighter Model - Final Report," General Electric Company - Pending.

10. Frost, T.H.,, "Practical Bypass Mixing Systems for Fan Jet Aero Engines," The Aeronautical Quarterly, May 1966, pp. 141-160.